Experimental validation of genome-environment associations in Arabidopsis

Yuxin Luo[1,2], Claire M. Lorts[1], Erica H. Lawrence-Paul[1], Jesse R. Lasky[1]

[1]Department of Biology, Pennsylvania State University

[2]Correspondence

Abstract

Identifying the genetic basis of local adaptation is a key goal in evolutionary biology. Allele frequency clines along environmental gradients, known as genotype-environment associations (GEA), are often used to detect potential loci causing local adaptation but are rarely followed by experimental validation. Here, we tested loci identified in three moisture-related GEA studies on *Arabidopsis*. We studied 42 GEA-identified genes using t-DNA knockout lines under drought and tested effects on flowering time, an adaptive trait, and genotype-by-environment (GxE) interactions on performance and fitness. In total, 16/42 genes had significant effects on traits involved in local adaptation or performance response to environment. We found that *wrky38* mutants had significant GxE effects for fitness; *lsd1* plants had a significant GxE effect for flowering time, while 11 genes showed flowering time effects with no drought interaction. However, most GEA candidates did not exhibit GxE. In the follow-up experiments, *wrky38* caused decreased stomatal conductance and specific leaf area under drought, indicating potentially adaptive drought avoidance. Additionally, GEA identified natural putative LoF variants of *WRKY38* associated with dry environments, as well as alleles associated with variation in *LSD1* expression. While only a few GEA-identified genes were validated for GxE interactions for fitness under drought, we likely overlooked some because experiments might not well represent natural environments and t-DNA insertions might not well represent natural alleles. Nevertheless, GEAs apparently identified some genes contributing to local adaptation. GEA and follow-up experiments are straightforward to implement in model systems and demonstrate prospects for GEA discovery of new local adaptations.

Keywords: Genome-environment associations (GEA); Drought stress; Local adaptation; t-DNA knockout; *WRKY38*; *LSD1*.

INTRODUCTION

A substantial portion of genetic variation within species in ecologically important traits is likely due to local adaptation to the environment (Savolainen et al., 2013; Tigano and Friesen, 2016; Wadgymar et al., 2022). Local adaptation is defined by a genotype-by-environment (GxE) interaction where local genotypes have higher fitness than foreign genotypes (Kawecki & Ebert, 2004). Identifying locally adaptive alleles and traits is of great interest in plant and animal breeding and conservation, where these alleles can be deployed for genetic improvement and prediction (Cortés et al., 2022; Crossa et al., 2017; Lasky et al., 2023; Whiting et al., 2024). Central questions of local adaptation include the effect size and number of involved mutations (Yeaman and Whitlock, 2011), whether locally adapted mutations have tradeoffs among different environments (Lee et al., 2024), whether the same or different mutations are involved in local adaptation to the same environments in different populations (Ralph and Coop, 2015), and which environmental gradients drive locally adaptive genetic variation (Lasky et al., 2012).

Conducting multiple common garden experiments to map populations and genetic loci contributing to fitness tradeoffs has been a gold standard approach (Clausen et al., 1941). However, such experiments are logistically challenging or impossible in many systems. Alternative approaches using geographic patterns in allele frequency have emerged for identifying loci potentially underlying local adaptation. Loci showing substantial allele frequency differences between populations, i.e. certain environment variables, may indicate those driving local adaptation (Coop et al., 2010; Endler, 1973). With the increasing availability of high-throughput genomic data, Genome-Environment Association (GEA) studies have been widely employed to identify putative locally adapted loci (Lasky et al., 2023; Rellstab et al., 2015).

GEAs employ diverse methods to identify loci where allele frequency is closely associated with environmental conditions (Lasky et al., 2023; Rellstab et al., 2015). Methods differ depending on whether they are single-locus or multi-loci (e.g. genome-wide) models (Betancourt et al., 2021; Gehan et al., 2015; Hager et al., 2022; Hancock et al., 2011; Lasky et al., 2012; Lee et al., 2024), where the latter may capture groups of loci covarying with the environment that are potentially relevant for polygenic adaptation (Forester et al., 2018). Additionally, there are methods that control for genome-wide patterns of similarity among populations using random effects (Zoubarev et al., 2012). While these approaches may reduce spurious associations due to population structure-environmental covariation, they can also be too conservative (Alonso-Blanco et al., 2016). Thirdly, some approaches synthesize the evidence from GEA with additional evidence, such as multiple common garden experiments (Capblancq et al., 2023; Lasky et al., 2018; Soudi et al., 2023). While these methods are now standard approaches in ecological genomics, the findings are rarely followed by experimental validation of variation at individual loci (Monroe et al., 2018; Nyine et al., 2025; Tergemina et al., 2025).

To experimentally test the hypothesis that variation at a given locus causes GxE for fitness, approaches that isolate experimental genetic variation to that locus are the most powerful. Creating near-isogenic lines (NILs) segregating at a given locus is ideal for testing GxE effects in a natural genetic background, but it is a time-consuming process. Gene knockout mutants in model species like *Arabidopsis* provide an alternative tool for testing GxE effects of variation at a particular gene. For example, various Arabidopsis knockout lines carrying t-DNA

insertions within genes that disrupt their function provide valuable resources for studying the effects of individual genes on fitness and other ecologically important traits. Although these mutants may not fully represent natural allelic variation for local adaptation, using them may be a good option for bulk experimental screening of candidate loci (Chong and Stinchcombe, 2019; Monroe et al., 2018). Resequencing of large numbers of natural *Arabidopsis* genotypes has yielded more detailed information on functional variation (Alonso-Blanco et al., 2016), which can be linked to loci of interest to make inferences about functional variants generating strong signals in GEA studies.

Arabidopsis thaliana is a small annual plant native to a wide range across Eurasia and Africa with diverse climates (Yim et al., 2024). Many studies have demonstrated potential drought adaptation of *A. thaliana* in quantitative traits (Dittberner et al., 2018), SNPs or genes (El-Soda et al., 2015; Exposito-Alonso et al., 2018; Hancock et al., 2011), and gene expression (Lasky et al., 2014). *A. thaliana* employs diverse strategies for drought adaptation such as drought escape via phenology, drought avoidance via traits reducing water loss, and drought tolerance via enhancing water acquisition or water-use efficiency (Lovell et al., 2013).

Here we focus on studying loci identified based on 3 different approaches, with the goal of testing whether identified genes indeed cause genotype-drought effects on fitness or other aspects of performance. We are also interested in whether the genes identified as drought-adapted in our experiments have allele frequency clines across the worldwide distribution of *A. thaliana*. For mutants identified as showing interesting genotype-environment interactions in our initial drought screen experiment, we followed up by testing their response to an additional, different drought treatment.

We tested the following hypotheses:

1. Some genes identified through GEA as potentially drought adapted exhibit natural variation in putative gene function assessed from resequencing data. Such genes would be especially amenable to using t-DNA knockout lines for testing the effects of natural variation. Mutations in genes without natural loss-of-function variation can still be assessed using t-DNA lines, though their relevance to natural variants is less clear.
2. Knockout mutants of these genes display significant genotype-drought interactions affecting traits (e.g. flowering time) known to be under changing selection in drought, fitness or performance traits in controlled drought experiments; and
3. These genes show climate-associated allelic variation and genomic signatures of selection, patterns consistent with adaptation to dry climates.

In our main drought screen, we found that *wrky38* had significant GxE effects on several fitness-related traits, and *lsd1* had a significant GxE effect on flowering time. Both *WRKY38* and *LSD1* were top candidates associated with moisture in their originated studies (Lasky et al., 2018, 2012). Additionally, *WRKY38* was also found most strongly associated with winter low temperatures in the combined common garden study (Lasky et al., 2018), while knockouts of *LSD1* were found to affect chilling sensitivity (Huang et al., 2010) and allelic variation was associated with the second principal component of climate (moisture related, Lee et al., 2017) in Arabidopsis. Both genes happen to play a role in the salicylic acid (SA) pathway (Bernacki et al., 2019; Kim et al., 2008; Szechyńska-Hebda et al., 2016; Wituszynska et al., 2013), primarily known for microbial defense response but which can be activated by abiotic stress (reviewed in Miura and Tada, 2014; Wu et al., 2019). Incorporating previous studies and our results, we

decided to use the two mutants to follow up with intermediate drought and freezing experiments, in order to test their possible adaptation in different drought and cold regimes in terms of their ecophysiological responses.

METHODS

Selecting genes from published genome-environment associations

We selected genes to test using five SNP lists from three published GEA studies that employed three different approaches. The first approach was based on mixed models of genome-wide associations with climate, where we included random effects to account for genomic similarity (Kang et al., 2008). For these mixed models, we calculated SNP associations with intra-annual monthly precipitation variability, growing season precipitation variability, or inter-annual growing season precipitation variability (i.e. 3 separate environmental GWAS, Lasky et al., 2014). We took the SNPs from all three climate associations and combined them into one list ranked by *p*-value for the mixed model association test. The second approach was a multivariate ordination where we identified SNPs most strongly associated with the first axis, which was associated with seasonality of temperature and precipitation, or the first axis after partialing out spatial variables, which was strongly associated with summer moisture (Lasky et al., 2012). We took SNPs with the strongest absolute loadings on each of these axes. The third approach was based on integrated information from four common gardens across Europe and also the broader ecotype panel to identify SNPs that showed the strongest SNP-climate associations and GxE for fitness favoring home climate alleles in monthly growing season precipitation variability or aridity index (i.e. annual precipitation/PET; Lasky et al., 2018). In total, we generated 1, 2, and 2 lists of SNPs from the three studies respectively.

From the top SNPs in each list, we only kept SNPs at least 250 kb apart. Starting from the SNP with the lowest *p*-values, we took up to 3 closest genes within 5kb of the SNP until we had at least 15 genes for each of the four lists of SNPs, or in the case of the combined climate association study, until we had at least 25 genes.

This procedure resulted in a list of 90 candidate genes. We chose 44 SALK lines representing knockouts of 42 genes, including 42 lines with insertions within exons and 2 lines with insertions within introns and confirmed homozygosity using tDNA Express: Arabidopsis Gene Mapping Tool (Alonso et al., 2003; Table S1). Among the 44 SALK lines targeting 42 genes, three lines (SALK_048316C, SALK_085852C, and SALK_063969) targeting AT5G65080 (*MAF5*) and AT3G45860 (*CRK4*), although not top candidates, were included in the experiment because their potential functional significance in drought adaptation (Kim and Sung, 2010; Ratcliffe et al., 2003; Zhao et al., 2023). As a result, 40 top-candidate genes were validated in this study.

Functional variation in the screened loci in the 1001 Genomes

We analyzed putative functional variation (hereafter FV) in the 1001 Genomes resequencing data for all genes screened. We used the 1001 Genomes Polymorphism Browser (https://tools.1001genomes.org/polymorph/) to identify potential large-effect mutations in each gene, which were considered as putative loss-of-function (LoF) mutations. If more than one isoform existed for a gene, we recorded the case of the most common isoform, except when no functional variant was found for this isoform, we instead used the most common isoform that had functional variants. We summarized the counts of each type of functional variation and the positions where the variations occurred.

Main drought screen

Detailed experimental settings are provided in Supplementary Methods. Briefly, we programmed the chamber temperature and photoperiod based on that of the *Lip-0* ecotype from southern Poland following Lorts and Lasky (2020) (Table S2). Each tray represented either a drought or well-watered treatment, and seven replicates per mutant were randomly assigned positions for each treatment. Seeds were stratified in DI water for 4-5 days prior to planting.

Pots were maintained at 2.5-5 cm of bottom water before drought treatments, which began 19 days post-planting. Bottom water was removed from drought trays, while well-watered trays retained a constant 2.5 cm of water and received 2.5 ml of top water every other day. After five weeks, all pots were top-watered with a 12 ml miracle grow solution every other day to ensure nutrition.

At maturity, fecundity was assessed when siliques dried and rosette leaves senesced. We recorded inflorescence height and secondary branch numbers were recorded. For reproductive fitness estimates, we measured total silique number and silique length for 6 siliques to calculate average silique length, then calculated the total silique length as the product of silique number and average silique length.

After measurements, aboveground dry biomass was obtained, and rosette tissue was ground for $\delta^{13}C$ and $\delta^{15}N$ isotope analysis. $\delta^{13}C$ represents estimate for water use efficiency (WUE).

Follow-up drought and freezing experiments

Intermediate drought experiment on *wrky38* and *lsd1*

For intermediate drought (ID), plants were grown at 20/14°C (12h/12h) with varying watering frequencies (every 3 days for well-watered, every 6 days for drought). We tracked stomatal conductance (g_{sw}) and Fv/Fm for 10 for four plants per genotype per treatment. Specific leaf area (SLA), relative water content (RWC), and leaf isotope analyses ($\delta^{13}C$, C:N and $\delta^{15}N$) were analyzed using five to six 40-day-old rosettes (see Supplementary Methods for details).

We recorded the flowering time for six replicates per genotype per treatment. As in the main drought screen, we measured the same growth and fitness traits and isotopes.

Overnight freezing experiment on *wrky38* and *lsd1*

Twelve replicates of *Col*, *wrky38*, and *lsd1* were grown at 20/14°C (12h/12h) until Day 30, then acclimated to 10/4℃ for 2 weeks before freezing treatment at 10/-2℃. We surrounded all pots with extra soil for insulation to prevent unnaturally soil freezing. On day 60, we measured diameter as an estimate of growth under freezing. After temperature was restored on Day 64, flowering time, biomass, silique traits, and inflorescence length were recorded as described above.

Statistical analyses

In both the drought experiments, we were primarily interested in whether the knockouts had genotype-specific drought responses, i.e., whether there were genotype-by-drought interactions, as well as whether the knockouts altered average phenotypes under drought, i.e., whether genotype effects were significant. Thus, we applied linear mixed models (LMMs) to test traits we measured between *Col* and each mutant separately, considering genotypes as fixed effects and tray numbers as random effects. To account for false positives arising from multiple LMMs within the dataset, we calculated adjusted *p*-values using a False Discovery Rate (FDR) threshold of 0.05, applying the *p.adjust()* function in R. We summarized how genes, originally identified in previous studies, were selected for knockout experiments and examined whether they exhibited significant genotype effects. Additionally, we calculated the ratio of genes tested with significant genotype effects relative to the total number of genes selected for screening in each original study. We also applied LMMs on the daily g_{sw} and Fv/Fm data measured in the ID experiment to detect if the mutants differed from *Col* in ecophysiology on any of the 10 measuring days.

It was not feasible to control moisture in the freezing experiment as we did in the drought follow-up because soil lost water much more slowly than it did in higher temperatures, so we used *DunnettTest()* function in the R package *DescTools* (Signorell et al., 2023) to conduct Dunnett's Test on traits measured in the freezing experiment, using *Col* as control and test for differences of the two mutants to control separately.

Population genetic variation at *WRKY38*

Because we found some putative LoF for *WRKY38* were relatively common in the 1001 Genomes accessions, we further analysed the geographic and genetic structure of these variants. We used the imputed SNP matrix (hdf5 file) and short indels (vcf file) downloaded from the 1001 Genome Project website (https://1001genomes.org/accessions.html) for the following analyses.

We calculated Tajima's D across chromosome 5 (Chr 5) in 5-kb windows using VCFtools (--TajimaD 5000) to test possible selection signals on *WRKY38* in natural accessions. The most common functional variant for *WRKY38* is a frameshift at position 7495793 on Chr 5 ($Frameshift_{7495793}$; Table S3). To detect linkage disequilibrium and potential haplotype structure (i.e. non-random associations among SNPs within the genomic region) between

236 Frameshift$_{7495793}$ and adjacent SNPs, we calculated the square of the Spearman's correlation
237 coefficient (r^2). This calculation was performed between the presence/absence of
238 Frameshift$_{7495793}$ and the alleles of each SNP within 5 kb upstream and downstream of *WRKY38*
239 using the *cor()* function in base R.
240 To characterize the geographic and population structure of natural putative LoF
241 mutations in 1001 Genomes accessions, we plotted mutations and their genetic clusters by
242 different shapes and outline colors on a map. We also constructed neighbor-joining (NJ) trees
243 built with the entire gene sequence of *WRKY38* (including coding and non-coding sequences),
244 and a genome-wide NJ tree. We referred to the population structure of 1001 Genomes
245 accessions in Alonso-Blanco et al. (2016), where the authors classified 9 genetic clusters and
246 one admixed group. For simplicity of data presentation, we combined the 9 groups by 5 major
247 regions — West Mediterranean (W-Med), North Mediterranean (N-Med), Central and Western
248 Europe (CW-Euro), North Europe (N-Euro), and Asia. Accessions that were introduced,
249 classified in the admixed group, or might be potential contaminations (Pisupati et al., 2017) were
250 not included in the 5 groups.
251 We used the R package *maps* to visualize the distribution of the common putative LoF
252 mutations of *WRKY38*. To build the genome-wide tree, we annotated the vcf file using SnpEff
253 (Cingolani et al., 2012), extracted the synonymous sites, filtered out sites with minor allele
254 frequency below 0.01 (--maf 0.01) and missing rate over 10% (--max-missing 0.9), and
255 generated a distance matrix using PLINK (Purcell et al., 2007). Both NJ trees were constructed
256 using the *nj()* function from package *ape* (Paradis and Schliep, 2019).
257 We hypothesized that the natural *WRKY38* putative LoF variants could underlie local
258 adaptation. To identify which climate variables might best explain *WRKY38* functional variation
259 and be most closely tied to mechanisms of selection, we used LMMs to scan for correlations
260 across the 19 bioclimatic variables. Worldclim 2 bioclimatic data were retrieved using the
261 *getData()* function from the R package raster (Fick and Hijmans, 2017; Hijmans et al., 2015).
262 Models were implemented using *coxme* and *kinship2* packages to include kinship in the models
263 as random effects (Sinnwell et al., 2014; Therneau and Therneau, 2015). We focused on testing
264 the local adaptation of intact *WRKY38*, Frameshift$_{7495793}$, the most common and widespread FV,
265 and Frameshift$_{7495793\&94}$, which accounted for a 3-bp frameshift that led back to the normal open
266 reading frame (ORF) thus suspected to be potentially functional. Since mixed models have low
267 power when causal variants are correlated with the genomic background, we also used Welch's
268 t-test (*t.test()*) in R to compare the differences in bioclimatic variables for accessions with/out the
269 intact gene or the FVs.

270 Variation in *LSD1* expression

271 Only 5 of the total 1135 accessions had *LSD1* putative LoF mutations. Thus, we suspected that
272 LoF may not be the major cause of the strong association between climate and the *LSD1*-
273 targeting SNP in Lasky et al. (2018), and the adaptation might exist due to amino acid changes
274 or *cis*-regulatory variation impacting expression. Therefore, we scanned across 19 bioclimatic
275 variables and SNPs (ref/alt alleles) within 10kb around *LSD1* using univariate GEAs with
276 GEMMA (Zoubarev et al., 2012) for 933 native accessions with known coordinates that were not
277 potential contaminants (Pisupati et al., 2017). We found elevated correlations with climate at

278 SNPs 1kb upstream of *LSD1* and the start of the gene sequence, suggesting that the adaptation
279 may occur at the promoter region. These SNPs may influence gene expression by altering
280 transcription factor binding motifs (Shastry, 2009; Wang et al., 2005).
281 Thus, we further asked if these SNPs impact *LSD1* expression using the published 1001
282 Genomes transcriptome data (http://signal.salk.edu/1001.php; Kawakatsu et al., 2016). Among
283 728 accessions with published transcriptome data, 1 accession was excluded from the following
284 analysis according to Pisupati et al. (2017). We compared the expression levels of *LSD1*
285 between the two alleles of the top climate-associated SNPs in the putative promoter region by
286 Welch's t-test (*t.test()*) in R. We also used linear models (*lm()*) to find possible associations
287 between *LSD1* expression and bioclimatic variables. Additionally, we investigated whether
288 SNPs with elevated correlations to climate are enriched in bioclimatic variables associated with
289 *LSD1* expression.

290 RESULTS

291 Widespread putative functional variation in the experimentally 292 screened genes in the 1001 Genomes accessions

293 Across all 1135 accessions, 1070 exhibit at least one high-impact functional variant (i.e. putative
294 LoF) over the 44 experimentally screened genes. Specifically, 1973 putative frameshifts
295 occurred in 943 genotypes as well as 1116 stop-gained FVs in 842 genotypes, appearing to be
296 the most prevalent types of putative high-impact variants over the identified genes (Table S3).
297 Splice donor variants were found in 303 accessions, and splice-acceptor, stop-lost, and start-
298 lost variants were found in 29, 5, and 4 accessions, respectively.
299 Putative frameshifts were most common in AT1G19410 (*FBD*), occurring in 639
300 accessions. Frameshift variants were also common in AT5G22570 (*WRKY38*), detected in 250
301 accessions. Stop-gained had the most counts in AT5G22900 (*CHX3*), with 492 accessions
302 having the putative FVs. Splice-donor was also the most prevalent in the *FBD* gene, exhibited
303 by 220 accessions. The rest of the high-impact effects were rare among the screened loci,
304 suggesting purifying selection on amino acid sequences. We found 14 accessions with splice-
305 acceptor variants, 2 accessions with stop-lost, and 2 accessions with start-lost at AT5G10960
306 (*CAF1I*), AT3G45860 (*CRK4*), and AT5G22570 (*WRKY38*), respectively.
307 Some mutations in the screened genes had potential dual effects, and such dual effects
308 were locusspecific. A 1-bp deletion or insertion at the same position in AT1G76090 (*SMT3*)
309 caused both frameshift and start-loss, resulting in the most common dual effects observed in 95
310 accessions. Two insertions in AT3G45860 (*CRK4*) could each lead to dual effects of frameshift
311 and stop-gain, together occurring in 21 accessions. In rare cases, a 1-bp deletion in
312 AT5G40830 (*ICA*) caused frameshift and stop-lost in 4 accessions, while a 3-bp deletion in
313 AT5G65050 (*AGL31*/*MAF2*) caused stop-lost and disruptive-inframe-deletion effects in 1
314 accession.

Prevalent treatment effects, variable genotype effects, and few GxE effects on fitness and phenology in the main drought screen

Drought treatment effects on phenotypes were strong and largely consistent across different t-DNA insertion lines (Figure 1). Specifically, the drought effects were significant with FDR=0.05 across all 44 tested lines, causing lower aboveground biomass, smaller inflorescence length and weight, fewer siliques, shorter average and total silique length, and delayed flowering, with line CS68738 (*lsd1*) being the only exception with no significant drought effect on flowering time (Figure 1). The drought effect on rosette weight was also common, significantly reducing rosette weights in 25 of 44 lines at FDR = 0.05.

Genotype effects varied across the 44 lines tested (Figure 1, Table S4-6). Genotype effects were most common for flowering time, with 20 having nominally significant effects (α = 0.05) on flowering, primarily accelerating flowering, except for *wrky38*, which exhibited delayed flowering under drought. Thirteen insertion lines were significant with FDR = 0.05 (12 accelerated flowering and 1 delayed flowering (*wrky38*). Rosette and inflorescence weights were the traits with the next most insertion lines with genotype effects, 14 lines having nominally significant effects and 5 significant at FDR = 0.05 that mostly led to increased rosette weight and reduced inflorescence weight. Genotype effects on other traits measured were less common, with 5,5,5,3,1 lines having nominally significant effects and 1,0,0,1,1 lines significant with FDR = 0.05 for silique number, average and total silique length, inflorescence length, and aboveground biomass, respectively.

We found few genotype-by-treatment interactions caused by the t-DNA insertions. CS864818, a *WRKY38* (AT5G22570) knockout line, was the only one having a GxE effect that was significant at FDR = 0.05 on inflorescence length, silique numbers, total silique length, aboveground biomass, and inflorescence weight (Table 1,S5-S6). Generally, *wrky38* showed less drought sensitivity than *Col* while being smaller and less fecund in well-watered conditions except that the mutant had slightly longer inflorescence lengths than *Col* (*wrky38*: 40.1±3.010 cm; *Col*: 36.0±0.713 cm; Figure 2). When considering only genotype effects, the knockout of *WRKY38* caused significantly later flowering, longer inflorescence, more siliques, and greater rosette weights (Figure 2, Table 1,S4-S6. However, under drought conditions, only flowering time and inflorescence length were significantly different from *Col*.

Another mutant, *lsd1*, was one of only two having nominally significant genotype-by-treatment interaction (GxTrt) on flowering time (p = 0.0015; the other line SALK_012432 had p = 0.0479). The mutation significantly accelerated flowering compared to *Col*, and its interaction with drought exacerbated early flowering (Table 1). Notably, the mutant flowered earlier than *Col* under both WW and drought conditions (WW: 58.1±1.06 vs. 58.6±0.972 days; drought: 52.3±3.58 vs. 68.1±1.94 days), and unlike *Col* the effect of drought on flowering time was not significant (p = 0.3981). Drought had significant effects on fitness-related traits that reduced silique numbers, average silique length, and total silique length while the GxTrt effects on fitness were generally not significant (Table 1,S4-S6). lsd1 plants had significantly lower inflorescence and rosette weights, thus lower aboveground biomass, compared to *Col* (Figure 2, Table 1,S4-S6).

Both genotypes had increased WUE under drought compared to WW conditions (Figure 2), with treatment effects on WUE significant in LMMs that include *Col* and each mutant (p_{wrky38}

= 9.33e-18, p_{lsd1} = 1.15e-6). The genotype effect of *WRKY38* knockout also significantly increased its WUE compared to *Col* (p = 8.81e-8), while that of *lsd1* was not significant (p = 0.756; Figure 2). *wrky38* had an increased $\delta^{15}N$ ratio under drought compared to the well-watered condition, but its responses under both conditions were not substantially different from *Col* (p_G = 0.5010, p_{Trt} = 0.5575; Figure 2). *lsd1* mutants, however, had $\delta^{15}N$ being lower under drought while slightly higher under WW compared to *Col* (p_G = 0.0387, p_{GxTrt} = 4.22e-4), suggesting a possible nitrogen source shift under drought. C:N ratios had been overall reduced under drought, probably the result of reduced biomass under drought (Figure 2).

Comparing candidates from different GEA approaches

We compared each approach in identifying genes that influence fitness and performance traits under drought, potentially indicating their role in drought adaptation. Among the 40 top-candidate genes from the original studies, 12, 12, 8, 6, and 7 genes were identified through RDA, partial RDA, univariate associations, the combined common garden approach with aridity index, and the combined common garden approach with monthly growing season precipitation, respectively (Table S1). Four genes were identified as top candidates by multiple approaches (Table S1). Among the knockout lines of these genes, only SALK_051689 (AT5G10960) had marginally significant genotype effect that accelerated flowering time (p_{adj} = 0.045, Table S5).

RDA and partial RDA proved to be the most effective methods for identifying drought-adapted genes, with each approach having 6 out of 12 genes exhibiting significant genotype effects at FDR = 0.05 across fitness and performance traits in the main drought screen. The combined common garden approach followed, with 2 out of 6 and 2 out of 7 genes identified via association with aridity index and monthly precipitation showing significant genotype effects at FDR = 0.05.

In contrast, none of the 8 genes identified by univariate associations showed significant genotype effects at FDR = 0.05, although 5 genes exhibited significant genotype effects at α = 0.05 before applying false discovery rate corrections.

Stable but less pronounced fitness, phenology, and ecophysiological responses of *wrky38* and *lsd1* under follow-up mild drought

Under the milder follow-up drought (ID), *wrky38* and *lsd1* plants also exhibited similar but less pronounced responses compared to those observed in the main drought screen. The mild drought significantly reduced fitness and inflorescence length across both *Col* and the mutants, as determined by mixed linear models that included *Col* and one mutant (*wrky38* or *lsd1*). Specifically, the drought significantly reduced fitness and inflorescence length for both *wrky38* and *lsd1*, while flowering time was not significantly impacted (Figure 3, Table 2,S7). Plants of *wrky38* mutants did not exhibit significant genotype-specific responses to drought compared to *Col* across the traits we measured (Table 2). However, the direction of *wrky38* differences was consistent with the earlier drought screen; e.g., *wrky38* had higher fitness and biomass than*Col* under drought, but the opposite under well-watered conditions (Figure 3). In contrast, *lsd1*

397 mutants showed significant genotype effects that reduce inflorescence length and total silique
398 length and a significant GxE effect for silique number (Table 2). This indicates that *lsd1* mutants
399 not only have reduced fitness under drought conditions, but the negative impact of drought was
400 even more pronounced in *lsd1* mutants compared to *Col*.
401 During the 10 days of ecophysiological tracking, we built LMMs to compare the daily g_{sw}
402 and Fv/Fm of the two mutants with *Col*. The stomatal conductance (g_{sw}) of all three genotypes
403 exhibited fluctuations that were associated with the regular watering schedule (Figure S1).
404 *wrky38* had potentially adaptive reduced g_{sw} compared to *Col* and under drought, with genotype
405 effects significant during the initial days of tracking, when drought-treated plants first
406 experienced water limitation (9 days after treatment initiation; Table S3). A significant GxE
407 interaction with drought was also observed (Table S8). The *lsd1* mutant also had reduced g_{sw}
408 under drought, but the genotype effect was insignificant (Figure S1; Table S8). None of the
409 Fv/Fm values we measured suggested major oxidative stress (Figure S2), coinciding with
410 Zivcak et al. (2013), indicating a mild drought. No genotype or treatment pattern was detected
411 for Fv/Fm.
412 The drought effect significantly reduced SLA when considering *Col* and *wrky38* but was
413 not significant in the model including *Col* and *lsd1* (Figure 3, Table 2). Genotype effects on SLA
414 were significant for both mutants, but *wrky38* had a lower SLA (potentially adaptive under
415 drought) while *lsd1* had a higher SLA compared to *Col* (Figure 3, Table 2). RWC exhibited little
416 variation between genotypes and treatments except for *lsd1* plants, which had a significant
417 genotype effect resulting in lower RWC (Table S7). The $\delta^{13}C$ response to treatment was
418 generally lower in the follow-up than in the main drought screen, indicating a milder drought in
419 the follow-up. The treatment effect on WUE was only significant for *wrky38* (p = 0.0029),
420 whereas the genotype effect on WUE was only significant for *lsd1* (p = 3.7e-4). No significant
421 GxE effects were detected for SLA, RWC, or $\delta^{13}C$ (Table S7).

422 Reduced vegetative growth or fitness of *wrky38* and *lsd1* under 423 overnight freezing

424 Treated with overnight freezing for 30 days, both *lsd1* and *wrky38* had significantly smaller
425 diameters than *Col* (p_{wrky38} = 0.0184, p_{lsd1} = 3.7e-4), representing their reduced vegetative
426 growth under low temperatures (Figure 4). After returning to warmer temperatures, we found no
427 variation in flowering time and silique number between *Col* and the two mutants. However, *lsd1*
428 had a shorter inflorescence length (p = 0.0360), average silique length (p = 0.0023), and total
429 silique length (p = 0.0218) than *Col*. Both *lsd1* and *wkry38* had smaller biomass than *Col* (p_{wrky38}
430 = 0.0026, p_{lsd1} = 2.6e-4), which might also be due to reduced vegetative growth. Overall, *lsd1*
431 plants had reduced growth and fitness compared to *Col* under freezing, consistent with findings
432 of Huang et al. (2010) that *lsd1* is chilling sensitive. Although putative LoF variants in *WRKY38*
433 were strongly associated with warm winter temperatures (Lasky et al. 2018), *WRKY38*
434 knockouts did not exhibit fitness differences compared to *Col*, though their vegetative growth
435 was inhibited by overnight freezing compared to *Col*.

WRKY38 allelic variation associated with climatic moisture and temperature

To evaluate potential selection on *WRKY38* and its surrounding genomic region, we analyzed SNP diversity patterns and examined allele associations indicating possible selection effects. The Tajima's D of the 5-kb window containing the *WRKY38* gene was above 0 (Tajima's D = 1.429) and is above the average of Chromosome 5 (average Tajima's D = 0.660), but it did not significantly deviate from the distribution of Tajima's D across the chromosome (*z*-score = 0.659; Figure S3). The overall r^2 between SNPs in 10 kb around *WRKY38* and the most common functional variant (Frameshift$_{7495793}$) also indicated some haplotype structure, with the frameshift having elevated correlations (r^2 >0.4) for SNPs located within 2 kb upstream of *WRKY38* and in the first 500 bp of the gene (also where the frameshift was located, maximum r^2 = 0.5104; Figure S4). However, this was not a dramatically long region of linkage, suggesting no evidence for a recent sweep (cf. the strong correlation observed with chr4:10999188 and other SNPs in a 300 kb window around *LSD1,* Lee et al., 2017). Nevertheless, the putative LoF mutations carried large numbers of alternate SNP alleles across the locus, indicating some divergence and linkage (Figure 5i,S5). The haplotype structure at *WRKY38* can also be seen in the *WRKY38* gene neighbor-joining tree. While the genome-wide NJ tree shows a star-like structure consistent with the recent expansion of Arabidopsis (Lee et al. 2017) with accessions clustered based on geography (Figure 5f), the *WRKY38* tree shows strong divergence between sequences with Frameshift$_{7495793}$ versus putative intact *WRKY38* sequences (Figure 5g,h). This allelic variation is segregated across diverse lineages, including the relicts (Figure 5a,b,c,f). Coincidentally, the rare FVs were all unique to their lineages, suggesting recent origins (Figure 5f; Table S9). In contrast to the widespread Frameshift$_{7495793}$, they might reflect newer local putative LoF mutations.

The gene tree of WRKY38 shows that alleles with the same functional variants exhibit similar haplotype patterns, regardless of their genetic cluster (Figure 5g,h). For example, although most N-Euro accessions are in the non-Frameshift$_{7495793}$ clade, all 12 N-Euro accessions having Frameshift$_{7495793}$ are in the Frameshift$_{7495793}$ clade, overlapping with W-Med, CW-Euro, and Asian accessions carrying this allele. The only accession having Frameshift$_{7495794}$ and the only one with Stop-lost$_{7495609}$ are both within Frameshift$_{7495793}$ clade, while the 6 accessions having Frameshift$_{7496041}$ and 2 accessions having Stop-gained$_{7496443}$, which are grouped at the same tip on the gene tree, only occurred in the non-Frameshift$_{7495793}$ clade.

Inconsistency between the genomewide and *WRKY38* gene tree confirmed *WRKY38* allelic variation independent of population genetic structure. Next, we investigated whether this variation is associated with climatic factors, particularly moisture and drought related variables. We did not find significant correlations at α = 0.05 between the frequency of Frameshift$_{7495793}$ (the most common FV) or Frameshift$_{7495793\&94}$ (the FV that putative restores the normal ORF) and the bioclimatic variables when considering kinship (Table S10), which coincided with the findings of Alonso-Blanco et al. (2016) that almost no SNPs are significantly correlated with climate in environmental GWAS at FDR = 0.05 after considering population structure for 1001 Genomes accessions. Despite this, without accounting for kinship, significant differentiation was detected at α = 0.05 for 11, 12, and 4 bioclimatic variables between accessions with and without intact *WRKY38*, Frameshift$_{7495793}$, and Frameshift$_{7495793\&94}$, respectively (Table S11). Among the

479 significant associations, precipitation of the warmest quarter (bio18) had the lowest p-values for
480 both intact *WRKY38* (p = 6.8e-10) and Frameshift$_{7495793}$ (p = 8.8e-9). Specifically, intact
481 *WRKY38* occurred more frequently in regions with wet summers, while Frameshift$_{7495793}$ was
482 more common in hot and dry regions, suggesting the drought adaptation of *WRKY38* putative
483 LoF. Frameshift$_{7495793\&94}$ (which has a net in-frame effect) was most significantly correlated with
484 higher isothermality (bio3; p = 3.7e-4), followed by higher mean temperature of the wettest
485 quarter (bio8; p = 6.4e-4).

486 *LSD1* allelic variation and expression associated with climatic 487 moisture and temperature

488 Mixed models (GEMMA) detected strong correlations between SNPs within 10kb around *LSD1*,
489 particularly for SNPs within 1 kb upstream and the first 500 bp of *LSD1*, and multiple bioclimatic
490 variables (Figure 6a). These SNPs, located in the promoter region of *LSD1*, may influence gene
491 expression by altering transcription factor binding motifs (Shastry, 2009; Wang et al., 2005).
492 Thus, we hypothesized that these SNPs might contribute to local adaptation via changes in
493 gene expression.
494 To validate the hypothesis, we picked a top climate-associate SNP (Chr4, position
495 11003866) from the 1 kb upstream region of *LSD1* and tested for *LSD1* expression differences
496 between ref/alt alleles. This SNP had the strongest correlation, indicated by the lowest p-value,
497 with precipitation of the warmest quarter (bio18; wald-p = 2.390e-41; Figure 6b), followed by the
498 minimum temperature of the driest quarter (bio9; wald-p = 2.140e-36; Figure 6c). We found that
499 the alternative allele corresponded to significantly lower *LSD1* expression compared to the
500 reference allele (p = 0.003; Figure 6d), suggesting a connection between lower *LSD1*
501 expression and hot and dry climates.
502 Using linear models, we found that *LSD1* expression was significantly greater for
503 genotypes from wetter summer climates (precipitation of the warmest quarter (p=8.683e-5) and
504 precipitation of the wettest month (p=0.039)). Across the 10 kb region around *LSD1*, 68 of the
505 201 SNPs were most strongly associated with bio18 (precipitation of the warmest quarter).
506 Moreover, when limiting to SNPs within 1kb upstream of *LSD1*, i.e. the region we thought to be
507 linked with *LSD1*, the ratio became 25 of 35 SNPs. The results indicated that *LSD1* might play a
508 role in local adaptation to moisture regimes by *cis*-regulatory variation.

509 DISCUSSION

510 Local adaptation is a major source of phenotypic variation within species, but traditional
511 methods of identifying locally adapted genes are logistically challenging. Genotype-environment
512 associations (GEA) offer an easy-to-implement tool to generate hypotheses about genes
513 involved in local adaptation, but most published results remain as untested hypotheses. Here
514 we screened 42 genes identified from genome-wide GEA studies and found at least two had
515 effects on environmental responses and physiology linked to drought adaptation, suggesting
516 potential local adaptations.

517 In our main drought experiment, among 42 potential drought-adapted genes detected
518 with 3 different GEA approaches, the tDNA knockout of *WRKY38* (detected with RDA, Lasky et
519 al., 2012) exhibited a significant GxE effect on fitness-related traits, and *lsd1* mutant (gene
520 detected with combined GEA-common garden synthesis, Lasky et al., 2018) had a significant
521 GxE effect on flowering time, which could potentially indicate variation in drought escape versus
522 drought avoidance (Lovell et al., 2013). Coincidentally, these genes were both the top (#1)
523 candidate genes with the strongest GEA in the studies used to select them. The physiological
524 effect of *wrky38* identified in the follow-up screening suggests mechanisms of drought
525 avoidance for *wrky38*, via reduced stomatal conductance and SLA. Furthermore, the high
526 frequency of putative natural loss-of-function alleles of *WRKY38* in Arabidopsis populations
527 found in the drier southern part of its range suggests potential local adaptation.

528 Genotype and genotype-by-enviroment effects on phenotypes

529 Although the screened genes were the ones with the largest effects in the original
530 studies, the GxE effects for fitness that were significant in the main drought screen were no
531 longer significant under the milder drought conditions of the follow-up ID experiment. Several
532 factors could impact the results. First, the milder conditions of the follow-up drought experiment
533 compared to the main drought screen may have reduced the G×E effect on fitness. Second,
534 over-simplified laboratory environments could lead to systematic bias in plant fitness (Anderson
535 et al., 2013). In natural environments, drought conditions are usually coupled with elevated
536 temperatures, a variable not accounted for in controlled experiments designed to isolate the
537 effects of a single environmental factor. In the laboratory, when only a single environmental
538 variable is changed between treatments, a conditional neutrality, that a gene has fitness
539 advantages under one treatment and is neutral under the other, can be more common
540 (Anderson et al., 2013). Lastly, the knockout alleles of a gene may not be the mechanism of
541 local adaptation in nature. Local adaptation may also occur through *cis*-regulatory effects on
542 gene expression (Hämälä et al., 2020; Lasky et al., 2014) or changes in amino acid sequences.
543 Therefore, when screening candidate genes for local adaptation, it is important to consider lines
544 with significant genotype effects alongside those showing significant G×E effects for fitness. As
545 G×E effects may not always be significant due to the factors discussed above, genotype effects
546 may still capture environment-associated differentiation.
547 Besides G×E effects on fitness, G×E effects on flowering time are also noteworthy when
548 assessing local adaptation to drought stress, as early flowering is a critical drought escape
549 strategy (Franks, 2011; Kenney et al., 2014). Chong and Stinchcombe (2019) reported
550 systematic directional effects of flowering time among randomly selected SALK lines. In their
551 study, 11 out of 27 lines under long-day conditions and 3 out of 27 lines under short-day
552 conditions exhibited significantly different flowering times compared to *Col*, with all showing
553 delayed flowering. However, in our main drought screen, 19 out of 20 lines with significant
554 genotype effects at $\alpha = 0.05$, and 12 out of 13 lines with significant genotype effects at FDR =
555 0.05, exhibited accelerated flowering (Figure 1, Table S6). Among these, *wrky38* was the only
556 line that showed delayed flowering (a potential drought avoidance strategy, Ludlow, 1989).
557 Since the genes we selected were candidates for drought adaptation, the accelerated flowering

558 observed in these lines may indicate their potential for drought adaptation via escape (Ludlow,
559 1989).
560 Though we only observed GxE for fitness in a small number of genes, evidence of
561 associations between their natural functional variation and moisture-related bioclimate variables
562 demonstrated the underlying biological bases of potential local adaptation of loci identified by
563 GEA. Setting up this screen was relatively easy due to the availability of existing tDNA
564 resources, making the approach an efficient way to identify and screen potential locally adapted
565 genes in model organisms where such resources are available or relatively easily generated.

566 Comparison of common GEA approaches

567 Since the advent of GEA, a wide variety of methods have been proposed (reviewed by
568 Rellstab et al., 2015). We tested candidates from three approaches here: multivariate ordination
569 (RDA) of genotype and environment (Forester et al., 2018; Lasky et al., 2012), univariate
570 climate mixed model associations (Lasky et al., 2014), and univariate climate models integrated
571 with fitness data from multiple common gardens (Lasky et al., 2018). Even considering lines
572 exhibiting significant genotype effects in addition to GxTrt effects, the number of positives
573 remains too small to definitely compare these statistical GEA approaches. While Lotterhos
574 (2023) recently criticized RDA as inappropriate for GEA due to a high false positive rate, the
575 author used arbitrary and uncalibrated significance thresholds. By contrast, Figure S8 in
576 Lotterhos (2023) showed that RDA was among the best methods based on the area under the
577 precision-recall curve (AUC-PR). Our results further support this, showing that RDA and partial
578 RDA had the highest rate of genes exhibiting significant genotype effects at FDR = 0.05,
579 followed by the combined common garden approach. In comparison, none of the tested genes
580 identified through univariate associations showed significant genotype effects at FDR = 0.05.
581 We propose that using ranked GEA results is more informative than focusing on arbitrary
582 significance thresholds; as mentioned previously, *WRKY38* and *LSD1* were the top-ranked loci
583 in their respective studies (RDA and combined GEA-common garden mixed models,
584 respectively; Lasky et al. 2012, 2018).

585 Potential mechanisms of drought adaptation at *WRKY38* and 586 *LSD1*

587 The two mutants presented opposite responses under drought. *wrky38* had a significantly
588 smaller SLA when compared to *Col* and when under drought, indicating how *wrky38* maintained
589 stable RWC under well-watered and drought conditions. *wrky38* mutants have reduced g_{sw},
590 SLA, and leaf area (result not shown) under drought in the follow-up experiment and increased
591 WUE in response to drought during both experiments (Figure 2-3), suggesting a drought-
592 avoidance strategy of natural *WRKY38* LoF genotypes. In contrast, *lsd1* had a larger SLA than
593 *Col*, thus potentially more water loss (Niinemets, 2001), which may result in its reduced RWC.
594 Instead, *lsd1* mutants showed stable accelerated flowering under drought in our two drought
595 experiments, indicating a drought-escape strategy.
596 *WRKY38* negatively regulates plant basal pathogen defense by suppressing
597 *PATHOGENESIS-RELATED GENE 1* (*PR1*) expression, a defense gene induced by salicylic

598 acid (SA) (Kim et al., 2008). Additionally, *WRKY38* is also involved in drought- and cold-related
599 responses in barley (Marè et al., 2004). Among *Arabidopsis WRKY* members that were also
600 acting in the SA pathway for plant basal defense responses (Salinas et al., 2024), *AtWRKY54*
601 and *AtWRKY70* were found to negatively impact osmotic tolerance by reducing stomatal closure
602 (Li et al., 2013), while *AtWRKY46* was found to regulate light-dependent stomatal opening in
603 guard cells (Ding et al., 2014). Based on previous studies and our findings, we hypothesize that
604 *WRKY38* inhibits stomatal closure. If so, the lower g_{sw} we found in knockouts could reduce
605 water loss through the stomata and enhance fitness under drought.
606 In 1001 Genome accessions, natural *WRKY38* LoF alleles were strongly associated with
607 lower July moisture compared to intact alleles. Despite this strong association, these putative
608 LoF alleles were not fixed or entirely absent in any region. Our population genetics analyses
609 revealed that LoF *WRKY38* exists across the entire distribution region of *A. thaliana* and in
610 every lineage group (Figure 5a-f). We suspected that the LoF of *WRKY38* might have originated
611 before the migration across Eurasia of *A. thaliana* and colonized drier regions during this
612 process. In both drought experiments, *wrky38* generally had lower fitness compared to *Col*
613 under well-watered conditions. However, *wrky38* maintained relatively stable fitness under
614 drought stress, while *Col* showed a substantial fitness decrease. The drought insensitivity of
615 *wrky38* may explain how natural LoF *WRKY38* dominates drier regions during migration.
616 The absence of LSD1 protein in *lsd1* mutants promotes the accumulation of SA
617 (Bernacki et al., 2021), which adversely affects plant development and reproduction while
618 accelerating flowering in Arabidopsis (Salinas et al., 2024). These findings explained the
619 consistent accelerated flowering behavior observed across our two drought experiments.
620 However, *lsd1* plants differed in their fitness responses to the long-term water deficiency of our
621 main drought screen and periodical moisture fluctuation in our follow-up experiments (Figure 2-
622 3). Specifically, *lsd1* mutants had similar fitness to *Col* under well-watered and drought in the
623 main experiment, but they were less fit than *Col* (i.e. genotype effect was significant) in the
624 follow-up. Previous laboratory studies have shown that *lsd1* exhibits similar survival and seed
625 production to the wild type under nonlethal water deficiency. However, under lethal drought
626 stress that caused complete mortality in wild-type plants, *lsd1* demonstrated a significantly
627 higher survival rate, albeit with reduced seed production. These findings suggest a trade-off
628 between survival and fecundity under severe stress in controlled laboratory conditions
629 (Szechyńska-Hebda et al., 2016; Wituszynska et al., 2013). When grown in the field, *lsd1*
630 mutants did not exhibit seed yield differences compared to the wild type (Bernacki et al., 2019;
631 Szechyńska-Hebda et al., 2016; Wituszynska et al., 2013). This could explain our finding that
632 the *LSD1* gene had lower expression in the hotter and drier regions, as reduced expression
633 could similarly mitigate fitness trade-offs, enhancing survival in stressful climates.

634 Freezing responses of *wrky38* and *lsd1*

635 We conducted the freezing experiment because both genes may also be involved in adaptation
636 to freezing stress. A SNP within the *WRKY38* coding region (Chr. 5, pos:7496047) was the top
637 candidate loci associated with temperature of the coldest month in Lasky et al. (2018), and
638 *LSD1* is associated with chilling sensitivity (Huang et al., 2010). Moreover, these two genes are
639 both in the salicylic acid (SA) pathway that can be activated by cold stress (Miura and Tada,

2014; Wu et al., 2019). *WRKY38* was positively regulated by SA (Kim et al., 2008) while *LSD1* conditionally regulated SA concentration with the existences of *ENHANCED DISEASE SUSCEPTIBILITY1* (*EDS1*) and *PHYTOALEXIN DEFICIENT4* (*PAD4*) (Bernacki et al., 2019; Szechyńska-Hebda et al., 2016; Wituszynska et al., 2013).

WRKY38 knockouts exhibited similar fitness to *Col* despite reduced vegetative growth after long-term overnight freezing (Figure 4). Considering that *WRKY38* was originally identified through RDA (Lasky et al., 2012), this finding suggests a potential role in multivariate adaptation. The LoF allele might be advantageous in drier and warmer climates, while the functional allele might be more beneficial in cooler and wetter climates. *LSD1* knockouts had significantly reduced vegetative growth and fitness under freezing, coincident with the findings of Huang et al. (2010). Both mutants exhibited some disadvantages under freezing conditions compared to *Col*, indicating possible links between the function of these genes and adaptation to cold climates. Although both drought and freezing conditions can limit water availability and there is overlap in some molecular pathways or responses to each set of conditions (Kim et al., 2024), here our results suggest the drought-adaptive variants are not cold-adapted.

Conclusion

In this study, we tested the potential role of 44 t-DNA knockout mutants of GEA-identified genes in adaptation to drought stress using common garden experiments. While most mutants did not exhibit significant G×E effects for flowering time, performance, or fitness, two knockouts, *wrky38* and *lsd1*, demonstrated evidence of drought adaptation in both the main drought screen and follow-up intermediate drought common gardens. Natural variation in the function or expression of these genes across a moisture gradient further supports the utility of GEA approaches for generating hypotheses, though further experiments are required to test hypotheses. Our findings highlight the promise of GEA methods for uncovering novel local adaptations to environmental stressors.

Acknowledgments

We thank Cody Depew for assistance in ordering knockout lines, Amanda Penn for assistance with experiments, and Diana Gamba and Yuxing Xu for assistance with computation. Funding was provided by NIH R35GM138300 to JRL.

References

Alonso, J.M., Stepanova, A.N., Leisse, T.J., Kim, C.J., Chen, H., Shinn, P., Stevenson, D.K., Zimmerman, J., Barajas, P., Cheuk, R., Gadrinab, C., Heller, C., Jeske, A., Koesema, E., Meyers, C.C., Parker, H., Prednis, L., Ansari, Y., Choy, N., Deen, H., Geralt, M., Hazari, N., Hom, E., Karnes, M., Mulholland, C., Ndubaku, R., Schmidt, I., Guzman, P., Aguilar-Henonin, L., Schmid, M., Weigel, D., Carter, D.E., Marchand, T., Risseeuw, E., Brogden, D., Zeko, A., Crosby, W.L., Berry, C.C., Ecker, J.R., 2003. Genome-Wide Insertional Mutagenesis of Arabidopsis thaliana. Science 301, 653–657. https://doi.org/10.1126/science.1086391

Alonso-Blanco, C., Andrade, J., Becker, C., Bemm, F., Bergelson, J., Borgwardt, K.M., Cao, J., Chae, E., Dezwaan, T.M., Ding, W., Ecker, J.R., Exposito-Alonso, M., Farlow, A., Fitz, J., Gan, X., Grimm, D.G., Hancock, A.M., Henz, S.R., Holm, S., Horton, M., Jarsulic, M., Kerstetter, R.A., Korte, A., Korte, P., Lanz, C., Lee, C.-R., Meng, D., Michael, T.P., Mott, R., Muliyati, N.W., Nägele, T., Nagler, M., Nizhynska, V., Nordborg, M., Novikova, P.Y., Picó, F.X., Platzer, A., Rabanal, F.A., Rodriguez, A., Rowan, B.A., Salomé, P.A., Schmid, K.J., Schmitz, R.J., Seren, Ü., Sperone, F.G., Sudkamp, M., Svardal, H., Tanzer, M.M., Todd, D., Volchenboum, S.L., Wang, C., Wang, G., Wang, X., Weckwerth, W., Weigel, D., Zhou, X., 2016. 1,135 Genomes Reveal the Global Pattern of Polymorphism in *Arabidopsis thaliana*. Cell 166, 481–491. https://doi.org/10.1016/j.cell.2016.05.063

Anderson, J.T., Lee, C.-R., Rushworth, C.A., Colautti, R.I., Mitchell-Olds, T., 2013. Genetic trade-offs and conditional neutrality contribute to local adaptation. Mol. Ecol. 22, 699–708. https://doi.org/10.1111/j.1365-294X.2012.05522.x

Bernacki, M.J., Czarnocka, W., Rusaczonek, A., Witoń, D., Kęska, S., Czyż, J., Szechyńska-Hebda, M., Karpiński, S., 2019. LSD1-, EDS1- and PAD4-dependent conditional correlation among salicylic acid, hydrogen peroxide, water use efficiency and seed yield in Arabidopsis thaliana. Physiol. Plant. 165, 369–382. https://doi.org/10.1111/ppl.12863

Bernacki, M.J., Rusaczonek, A., Czarnocka, W., Karpiński, S., 2021. Salicylic Acid Accumulation Controlled by LSD1 Is Essential in Triggering Cell Death in Response to Abiotic Stress. Cells 10, 962. https://doi.org/10.3390/cells10040962

Betancourt, N.J., Rajpurohit, S., Durmaz, E., Fabian, D.K., Kapun, M., Flatt, T., Schmidt, P., 2021. Allelic polymorphism at foxo contributes to local adaptation in Drosophila melanogaster. Mol. Ecol. 30, 2817–2830. https://doi.org/10.1111/mec.15939

Capblancq, T., Lachmuth, S., Fitzpatrick, M.C., Keller, S.R., 2023. From common gardens to candidate genes: exploring local adaptation to climate in red spruce. New Phytol. 237, 1590–1605. https://doi.org/10.1111/nph.18465

Chong, V.K., Stinchcombe, J.R., 2019. Evaluating Population Genomic Candidate Genes Underlying Flowering Time in *Arabidopsis thaliana* Using T-DNA Insertion Lines. J. Hered. 110, 445–454. https://doi.org/10.1093/jhered/esz026

Cingolani, P., Platts, A., Wang, L.L., Coon, M., Nguyen, T., Wang, L., Land, S.J., Lu, X., Ruden, D.M., 2012. A program for annotating and predicting the effects of single nucleotide polymorphisms, SnpEff: SNPs in the genome of Drosophila melanogaster strain w1118; iso-2; iso-3. Fly (Austin) 6, 80–92. https://doi.org/10.4161/fly.19695

Clausen, J., Keck, D.D., Hiesey, W.M., 1941. Regional Differentiation in Plant Species. Am. Nat. 75, 231–250.

Coop, G., Witonsky, D., Di Rienzo, A., Pritchard, J.K., 2010. Using Environmental Correlations to Identify Loci Underlying Local Adaptation. Genetics 185, 1411–1423. https://doi.org/10.1534/genetics.110.114819

Cortés, A.J., López-Hernández, F., Blair, M.W., 2022. Genome–Environment Associations, an Innovative Tool for Studying Heritable Evolutionary Adaptation in Orphan Crops and Wild Relatives. Front. Genet. 13. https://doi.org/10.3389/fgene.2022.910386

Crossa, J., Pérez-Rodríguez, P., Cuevas, J., Montesinos-López, O., Jarquín, D., Campos, G. de los, Burgueño, J., González-Camacho, J.M., Pérez-Elizalde, S., Beyene, Y., Dreisigacker, S., Singh, R., Zhang, X., Gowda, M., Roorkiwal, M., Rutkoski, J., Varshney, R.K., 2017. Genomic Selection in Plant Breeding: Methods, Models, and Perspectives. Trends Plant Sci. 22, 961–975. https://doi.org/10.1016/j.tplants.2017.08.011

Ding, Z.J., Yan, J.Y., Xu, X.Y., Yu, D.Q., Li, G.X., Zhang, S.Q., Zheng, S.J., 2014. Transcription factor WRKY46 regulates osmotic stress responses and stomatal movement independently in Arabidopsis. Plant J. 79, 13–27. https://doi.org/10.1111/tpj.12538

Dittberner, H., Korte, A., Mettler-Altmann, T., Weber, A.P.M., Monroe, G., de Meaux, J., 2018. Natural variation in stomata size contributes to the local adaptation of water-use efficiency in *Arabidopsis thaliana*. Mol. Ecol. 27, 4052–4065. https://doi.org/10.1111/mec.14838

El-Soda, M., Kruijer, W., Malosetti, M., Koornneef, M., Aarts, M.G.M., 2015. Quantitative trait loci and candidate genes underlying genotype by environment interaction in the response of Arabidopsis thaliana to drought. Plant Cell Environ. 38, 585–599. https://doi.org/10.1111/pce.12418

Endler, J.A., 1973. Gene Flow and Population Differentiation. Science 179, 243–250. https://doi.org/10.1126/science.179.4070.243

Exposito-Alonso, M., Vasseur, F., Ding, W., Wang, G., Burbano, H.A., Weigel, D., 2018. Genomic basis and evolutionary potential for extreme drought adaptation in Arabidopsis thaliana. Nat. Ecol. Evol. 2, 352–358. https://doi.org/10.1038/s41559-017-0423-0

Fick, S.E., Hijmans, R.J., 2017. WorldClim 2: new 1-km spatial resolution climate surfaces for global land areas. Int. J. Climatol. 37, 4302–4315. https://doi.org/10.1002/joc.5086

Forester, B.R., Lasky, J.R., Wagner, H.H., Urban, D.L., 2018. Comparing methods for detecting multilocus adaptation with multivariate genotype–environment associations. Mol. Ecol. 27, 2215–2233. https://doi.org/10.1111/mec.14584

Franks, S.J., 2011. Plasticity and evolution in drought avoidance and escape in the annual plant Brassica rapa. New Phytol. 190, 249–257. https://doi.org/10.1111/j.1469-8137.2010.03603.x

Gehan, M.A., Park, S., Gilmour, S.J., An, C., Lee, C.-M., Thomashow, M.F., 2015. Natural variation in the C-repeat binding factor cold response pathway correlates with local adaptation of Arabidopsis ecotypes. Plant J. 84, 682–693. https://doi.org/10.1111/tpj.13027

Hager, E.R., Harringmeyer, O.S., Wooldridge, T.B., Theingi, S., Gable, J.T., McFadden, S., Neugeboren, B., Turner, K.M., Jensen, J.D., Hoekstra, H.E., 2022. A chromosomal inversion contributes to divergence in multiple traits between deer mouse ecotypes. Science 377, 399–405. https://doi.org/10.1126/science.abg0718

Hämälä, T., Gorton, A.J., Moeller, D.A., Tiffin, P., 2020. Pleiotropy facilitates local adaptation to distant optima in common ragweed (Ambrosia artemisiifolia). PLOS Genet. 16, e1008707. https://doi.org/10.1371/journal.pgen.1008707

Hancock, A.M., Brachi, B., Faure, N., Horton, M.W., Jarymowycz, L.B., Sperone, F.G., Toomajian, C., Roux, F., Bergelson, J., 2011. Adaptation to Climate Across the Arabidopsis thaliana Genome. Science 334, 83–86. https://doi.org/10.1126/science.1209244

Hijmans, R.J., Van Etten, J., Cheng, J., Mattiuzzi, M., Sumner, M., Greenberg, J.A., Lamigueiro, O.P., Bevan, A., Racine, E.B., Shortridge, A., 2015. Package ‘raster.’ R Package 734, 473.

Huang, X., Li, Y., Zhang, X., Zuo, J., Yang, S., 2010. The Arabidopsis LSD1 gene plays an important role in the regulation of low temperature-dependent cell death. New Phytol. 187, 301–312. https://doi.org/10.1111/j.1469-8137.2010.03275.x

Kang, H.M., Zaitlen, N.A., Wade, C.M., Kirby, A., Heckerman, D., Daly, M.J., Eskin, E., 2008. Efficient Control of Population Structure in Model Organism Association Mapping. Genetics 178, 1709–1723. https://doi.org/10.1534/genetics.107.080101

Kawakatsu, T., Huang, S.C., Jupe, F., Sasaki, E., Schmitz, R.J., Urich, M.A., Castanon, R., Nery, J.R., Barragan, C., He, Y., 2016. Epigenomic diversity in a global collection of Arabidopsis thaliana accessions. Cell 166, 492–505.

Kenney, A.M., McKay, J.K., Richards, J.H., Juenger, T.E., 2014. Direct and indirect selection on flowering time, water-use efficiency (WUE, δ13C), and WUE plasticity to drought in Arabidopsis thaliana. Ecol. Evol. 4, 4505–4521. https://doi.org/10.1002/ece3.1270

Kim, D.-H., Sung, S., 2010. The Plant Homeo Domain finger protein, VIN3-LIKE 2, is necessary for photoperiod-mediated epigenetic regulation of the floral repressor, MAF5. Proc. Natl. Acad. Sci. 107, 17029–17034. https://doi.org/10.1073/pnas.1010834107

Kim, J.-S., Kidokoro, S., Yamaguchi-Shinozaki, K., Shinozaki, K., 2024. Regulatory networks in plant responses to drought and cold stress. Plant Physiol. 195, 170–189. https://doi.org/10.1093/plphys/kiae105

Kim, K.C., Lai, Z., Fan, B., Chen, Z., 2008. Arabidopsis WRKY38 and WRKY62 transcription factors interact with histone deacetylase 19 in basal defense. Plant Cell 20, 2357–2371. https://doi.org/10.1105/tpc.107.055566

Lasky, J.R., Des Marais, D.L., Lowry, D.B., Povolotskaya, I., McKay, J.K., Richards, J.H., Keitt, T.H., Juenger, T.E., 2014. Natural Variation in Abiotic Stress Responsive Gene Expression and Local Adaptation to Climate in Arabidopsis thaliana. Mol. Biol. Evol. 31, 2283–2296. https://doi.org/10.1093/molbev/msu170

Lasky, J.R., Des Marais, D.L., McKAY, J.K., Richards, J.H., Juenger, T.E., Keitt, T.H., 2012. Characterizing genomic variation of Arabidopsis thaliana: the roles of geography and climate. Mol. Ecol. 21, 5512–5529. https://doi.org/10.1111/j.1365-294X.2012.05709.x

Lasky, J.R., Forester, B.R., Reimherr, M., 2018. Coherent synthesis of genomic associations with phenotypes and home environments. Mol. Ecol. Resour. 18, 91–106. https://doi.org/10.1111/1755-0998.12714

Lasky, J.R., Josephs, E.B., Morris, G.P., 2023. Genotype–environment associations to reveal the molecular basis of environmental adaptation. Plant Cell 35, 125–138. https://doi.org/10.1093/plcell/koac267

Lee, C.-R., Svardal, H., Farlow, A., Exposito-Alonso, M., Ding, W., Novikova, P., Alonso-Blanco, C., Weigel, D., Nordborg, M., 2017. On the post-glacial spread of human commensal Arabidopsis thaliana. Nat. Commun. 8, 14458. https://doi.org/10.1038/ncomms14458

Lee, G., Sanderson, B.J., Ellis, T.J., Dilkes, B.P., McKay, J.K., Ågren, J., Oakley, C.G., 2024. A large-effect fitness trade-off across environments is explained by a single mutation affecting cold acclimation. Proc. Natl. Acad. Sci. 121, e2317461121. https://doi.org/10.1073/pnas.2317461121

Li, J., Besseau, S., Törönen, P., Sipari, N., Kollist, H., Holm, L., Palva, E.T., 2013. Defense-related transcription factors WRKY70 and WRKY54 modulate osmotic stress tolerance by regulating stomatal aperture in Arabidopsis. New Phytol. 200, 457–472. https://doi.org/10.1111/nph.12378

Lorts, C.M., Lasky, J.R., 2020. Competition × drought interactions change phenotypic plasticity and the direction of selection on Arabidopsis traits. New Phytol. 227, 1060–1072. https://doi.org/10.1111/nph.16593

Lotterhos, K.E., 2023. The paradox of adaptive trait clines with nonclinal patterns in the underlying genes. Proc. Natl. Acad. Sci. 120, e2220313120. https://doi.org/10.1073/pnas.2220313120

Lovell, J.T., Juenger, T.E., Michaels, S.D., Lasky, J.R., Platt, A., Richards, J.H., Yu, X., Easlon, H.M., Sen, S., McKay, J.K., 2013. Pleiotropy of FRIGIDA enhances the potential for multivariate adaptation. Proc. R. Soc. B Biol. Sci. 280, 20131043. https://doi.org/10.1098/rspb.2013.1043

Ludlow, M.M., 1989. Strategies of response to water stress. In K. H. Kreeb, H. Richter, & T. M. Hinckley (Eds.), Structural and Functional Responses to Environmental Stresses (pp. 269–281). SPB Academic.

Luo, Y.; Lorts, C.M.; Lawrence-Paul, E.; Lasky, J.R. (Forthcoming 2025). Dataset from Experimental validation of genome-environment associations in Arabidopsis [Dataset]. Dryad. https://doi.org/10.5061/dryad.qrfj6q5s4

Marè, C., Mazzucotelli, E., Crosatti, C., Francia, E., Stanca, A. ?michele, Cattivelli, L., 2004. Hv-WRKY38: a new transcription factor involved in cold- and drought-response in barley. Plant Mol. Biol. 55, 399–416. https://doi.org/10.1007/s11103-004-0906-7

Miura, K., Tada, Y., 2014. Regulation of water, salinity, and cold stress responses by salicylic acid. Front. Plant Sci. 5.

Monroe, J.G., Powell, T., Price, N., Mullen, J.L., Howard, A., Evans, K., Lovell, J.T., McKay, J.K., 2018. Drought adaptation in Arabidopsis thaliana by extensive genetic loss-of-function. eLife 7, e41038. https://doi.org/10.7554/eLife.41038

Niinemets, Ü., 2001. Global-Scale Climatic Controls of Leaf Dry Mass Per Area, Density, and Thickness in Trees and Shrubs. Ecology 82, 453–469. https://doi.org/10.1890/0012-9658(2001)082[0453:GSCCOL]2.0.CO;2

Nyine, M., Davidson, D., Adhikari, E., Clinesmith, M., Wang, H., Akhunova, A., Fritz, A., Akhunov, E., 2025. Genomic signals of ecogeographic adaptation in a wild relative are associated with improved wheat performance under drought stress. Genome Biology 26, 35. https://doi.org/10.1186/s13059-025-03500-1

Paradis, E., Schliep, K., 2019. ape 5.0: an environment for modern phylogenetics and evolutionary analyses in R. Bioinformatics 35, 526–528.

Pisupati, R., Reichardt, I., Seren, Ü., Korte, P., Nizhynska, V., Kerdaffrec, E., Uzunova, K., Rabanal, F.A., Filiault, D.L., Nordborg, M., 2017. Verification of Arabidopsis stock collections using SNPmatch, a tool for genotyping high-plexed samples. Sci. Data 4, 170184. https://doi.org/10.1038/sdata.2017.184

Purcell, S., Neale, B., Todd-Brown, K., Thomas, L., Ferreira, M.A., Bender, D., Maller, J., Sklar, P., De Bakker, P.I., Daly, M.J., 2007. PLINK: a tool set for whole-genome association and population-based linkage analyses. Am. J. Hum. Genet. 81, 559–575.

Ralph, P.L., Coop, G., 2015. Convergent Evolution During Local Adaptation to Patchy Landscapes. PLOS Genet. 11, e1005630. https://doi.org/10.1371/journal.pgen.1005630

Ratcliffe, O.J., Kumimoto, R.W., Wong, B.J., Riechmann, J.L., 2003. Analysis of the Arabidopsis MADS AFFECTING FLOWERING Gene Family: MAF2 Prevents Vernalization by Short Periods of Cold [W]. Plant Cell 15, 1159–1169. https://doi.org/10.1105/tpc.009506

Rellstab, C., Gugerli, F., Eckert, A.J., Hancock, A.M., Holderegger, R., 2015. A practical guide to environmental association analysis in landscape genomics. Mol. Ecol. 24, 4348–4370. https://doi.org/10.1111/mec.13322

Salinas, P., Velozo, S., Herrera-Vásquez, A., 2024. Salicylic acid accumulation: emerging molecular players and novel perspectives on plant development and nutrition. J. Exp. Bot. erae309. https://doi.org/10.1093/jxb/erae309

Savolainen, O., Lascoux, M., Merilä, J., 2013. Ecological genomics of local adaptation. Nat. Rev. Genet. 14, 807–820. https://doi.org/10.1038/nrg3522

Shastry, B.S., 2009. SNPs: Impact on Gene Function and Phenotype, in: Komar, A.A. (Ed.), Single Nucleotide Polymorphisms: Methods and Protocols. Humana Press, Totowa, NJ, pp. 3–22. https://doi.org/10.1007/978-1-60327-411-1_1

Signorell, A., Aho, K., Alfons, A., Anderegg, N., Aragon, T., Arppe, A., Baddeley, A., Barton, K., Bolker, B., Borchers, H., 2023. DescTools: tools for descriptive statistics. R package version 0.99. 26. Compr. R. Arch Netw 289–291.

Sinnwell, J.P., Therneau, T.M., Schaid, D.J., 2014. The kinship2 R package for pedigree data. Hum. Hered. 78, 91–93.

Soudi, S., Jahani, M., Todesco, M., Owens, G.L., Bercovich, N., Rieseberg, L.H., Yeaman, S., 2023. Repeatability of adaptation in sunflowers reveals that genomic regions harbouring inversions also drive adaptation in species lacking an inversion. eLife 12, RP88604. https://doi.org/10.7554/eLife.88604

Szechyńska-Hebda, M., Czarnocka, W., Hebda, M., Karpiński, S., 2016. PAD4, LSD1 and EDS1 regulate drought tolerance, plant biomass production, and cell wall properties. Plant Cell Rep. 35, 527–539. https://doi.org/10.1007/s00299-015-1901-y

Tergemina, E., Ansari, S., Salt, D.E., Hancock, A.M., 2025. Multiple independent MGR5 alleles contribute to a clinal pattern in leaf magnesium across the distribution of Arabidopsis thaliana. New Phytol. n/a. https://doi.org/10.1111/nph.70069

Therneau, T.M., Therneau, M.T.M., 2015. Package ‘coxme’. R Package Version 2.

Tigano, A., Friesen, V.L., 2016. Genomics of local adaptation with gene flow. Mol. Ecol. 25, 2144–2164. https://doi.org/10.1111/mec.13606

Wadgymar, S.M., DeMarche, M.L., Josephs, E.B., Sheth, S.N., Anderson, J.T., 2022. Local Adaptation: Causal Agents of Selection and Adaptive Trait Divergence. Annu. Rev. Ecol. Evol. Syst. 53, 87–111. https://doi.org/10.1146/annurev-ecolsys-012722-035231

Wang, X., Tomso, D.J., Liu, X., Bell, D.A., 2005. Single nucleotide polymorphism in transcriptional regulatory regions and expression of environmentally responsive genes. Toxicol. Appl. Pharmacol., Living in a Safe Chemical World. Proceedings of the 10th International Congress of Toxicology 11-15 July, 2004, Tampere, Finland 207, 84–90. https://doi.org/10.1016/j.taap.2004.09.024

Whiting, J.R., Booker, T.R., Rougeux, C., Lind, B.M., Singh, P., Lu, M., Huang, K., Whitlock, M.C., Aitken, S.N., Andrew, R.L., Borevitz, J.O., Bruhl, J.J., Collins, T.L., Fischer, M.C., Hodgins, K.A., Holliday, J.A., Ingvarsson, P.K., Janes, J.K., Khandaker, M., Koenig, D., Kreiner, J.M., Kremer, A., Lascoux, M., Leroy, T., Milesi, P., Murray, K.D., Pyhäjärvi, T., Rellstab, C., Rieseberg, L.H., Roux, F., Stinchcombe, J.R., Telford, I.R.H., Todesco, M., Tyrmi, J.S., Wang, B., Weigel, D., Willi, Y., Wright, S.I., Zhou, L., Yeaman, S., 2024. The genetic architecture of repeated local adaptation to climate in distantly related plants. Nat. Ecol. Evol. 8, 1933–1947. https://doi.org/10.1038/s41559-024-02514-5

Wijfjes, R. Y., Boesten, R., Becker, F.F. M., Theeuwen, T.P.J.M., Snoek, B.L., Mastoraki, M., Verheijen, J.J., Güvencli, N., Denkers, L.-A.M., Koornneef, M., van Eeuwijk, F.A., Smit, S., de Ridder, D., Aarts, M.G.M., 2024. Allelic variants confer Arabidopsis adaptation to small regional environmental differences. Plant J. 120, 1662–1681. https://doi.org/10.1111/tpj.17067

Wituszynska, W., Slesak, I., Vanderauwera, S., Szechynska-Hebda, M., Kornas, A., Van Der Kelen, K., Mühlenbock, P., Karpinska, B., Mackowski, S., Van Breusegem, F., Karpinski, S., 2013. Lesion simulating disease1, enhanced disease susceptibility1, and phytoalexin deficient4 conditionally regulate cellular signaling homeostasis, photosynthesis, water use efficiency, and seed yield in Arabidopsis. Plant Physiol. 161, 1795–1805. https://doi.org/10.1104/pp.112.208116

Wu, Z., Han, S., Zhou, H., Tuang, Z.K., Wang, Y., Jin, Y., Shi, H., Yang, W., 2019. Cold stress activates disease resistance in Arabidopsis thaliana through a salicylic acid dependent pathway. Plant Cell Environ. 42, 2645–2663. https://doi.org/10.1111/pce.13579

Yeaman, S., Whitlock, M.C., 2011. THE GENETIC ARCHITECTURE OF ADAPTATION UNDER MIGRATION–SELECTION BALANCE. Evolution 65, 1897–1911. https://doi.org/10.1111/j.1558-5646.2011.01269.x

Yim, C., Bellis, E.S., DeLeo, V.L., Gamba, D., Muscarella, R., Lasky, J.R., 2024. Climate biogeography of Arabidopsis thaliana: Linking distribution models and individual variation. J. Biogeogr. 51, 560–574. https://doi.org/10.1111/jbi.14737

Zhao, M., Li, M., Huang, M., Liang, C., Chen, D., Hwang, I., Zhang, W., Wang, M., 2023. The cysteine-rich receptor-like kinase CRK4 contributes to the different drought stress response between Columbia and Landsberg erecta. Plant Cell Environ. 46, 3258–3272. https://doi.org/10.1111/pce.14665

Zivcak, M., Brestic, M., Balatova, Z., Drevenakova, P., Olsovska, K., Kalaji, H.M., Yang, X., Allakhverdiev, S.I., 2013. Photosynthetic electron transport and specific photoprotective responses in wheat leaves under drought stress. Photosynth. Res. 117, 529–546. https://doi.org/10.1007/s11120-013-9885-3

Zoubarev, A., Hamer, K.M., Keshav, K.D., McCarthy, E.L., Santos, J.R.C., Van Rossum, T., McDonald, C., Hall, A., Wan, X., Lim, R., Gillis, J., Pavlidis, P., 2012. Gemma: a resource for the reuse, sharing and meta-analysis of expression profiling data. Bioinformatics 28, 2272–2273. https://doi.org/10.1093/bioinformatics/bts430

Captions

Figure 1 Reaction norms (lines) and average trait values (boxes) of a subset of traits measured during the main drought screen across all 44 mutants and *Col*, with *Col*, *lsd1* (CS68738), and *wrky38* (CS864818) highlighted. Each line connects the average trait values of one genotype under well-watered (WW) and drought (D) treatments, with *Col*, *lsd1* (CS68738), and *wrky38* (CS864818) highlighted. Mutants showing significant genotype effects at FDR = 0.05 from linear mixed models (LMMs) comparing *Col* and one mutant are indicated by dashed lines.

Figure 2 A subsetof the traits measured during the main drought screen of *Col*, *lsd1* (CS68738), and *wrky38* (CS864818). Text annotations on the box plots indicate the significance of genotype (G), treatment (E), and genotype-treatment interaction (G×E) effects at $\alpha = 0.05$, based on LMMs comparing *Col* and one mutant. The text color denotes the mutant genotype. Significance levels are represented as follows: *, $0.01 \leq p < 0.05$; **, $0.001 \leq p < 0.01$; ***, $p < 0.001$.

Figure 3 Traits measured in the follow-up intermediate drought experiment of *Col*, *lsd1* (CS68738), and *wrky38* (CS864818). Text annotations on the box plots indicate the significance of genotype (G), treatment (E), and genotype-treatment interaction (G×E) effects at $\alpha = 0.05$, based on LMMs comparing *Col* and one mutant genotype. The text color denotes the mutant genotype. Significance levels are represented as follows: *, $0.01 \leq p < 0.05$; **, $0.001 \leq p < 0.01$; ***, $p < 0.001$.

Figure 4 Traits measured in the follow-up freezing experiment of *Col*, *lsd1* (CS68738), and *wrky38* (CS864818). Asterisks indicate significant trait differences between *Col* and each mutant based on Dunnett's test: *, $0.01 \leq p < 0.05$; **, $0.001 \leq p < 0.01$; ***, $p < 0.001$.

Figure 5 Natural variation of *WRKY38* putative LoF in the 1001 Genomes accessions. **a**, distribution of native *Arabidopsis* accessions from 1001 Genomes. Colors indicate ADMIXTURE genetic clusters, originally defined by Alonso-Blanco et al. (2016) and modified in this study. Accessions with clearly assigned genetic clusters are represented by filled icons in their respective cluster colors, while admixed accessions are shown with unfilled icons. **b**-**e**, distributions of natural *WRKY38* putative functional variation: **b**, distribution of accessions with intact *WRKY38*; **c**, distribution of accessions with $\text{Frameshift}_{7495793}$, the most common FV of *WRKY38* ; **d**, distribution of accessions with $\text{Frameshift}_{7495793\&94}$, a mutation that restores the

964 normal open reading frame; **e**, distribution of accessions with other rare FVs of *WRKY38*. **f,**
965 *WRKY38* FVs on the genomewide NJ tree, the relict lineage (Alonso-Blanco et al., 2016) was
966 marked by an arrow. **g**, *WRKY38* FVs on the NJ gene tree, symbols as in (**f**). **h,**
967 Frameshift$_{7495793}$ on the NJ gene tree. **i**, numbers of alternative SNPs in accessions with intact
968 *WRKY38* and putative LoF FVs within 10 kb around *WRKY38*. The number of accessions with
969 each type of functional variation is indicated in parentheses.
970 **Figure 6** Genotype-environment associations and *LSD1* expression. **a**, Scanning the *LSD1*
971 region to identify potential SNP-environment associations using LMM within 10kb. Each point
972 represents the smallest p-value from the 19 associations between each SNP and the 19
973 bioclimate variables. *LSD1* gene region is shown between the dashed lines. These associations
974 are meant to identify where in the locus variation is most strongly associated with climate. **b**, the
975 difference in precipitation of the warmest quarter (bio18) between reference and alternative
976 alleles at a top climate-associated SNP (Chr4, position 11003866). **c**, the difference in the
977 minimum temperature of the driest quarter (bio9) at an SNP (Chr4, position 11003866). **d**, the
978 difference in *LSD1* expression at an SNP (Chr4, position 11003866). **b-d**, asterisks indicate
979 significant trait differences from t-test: *, $0.01 \leq p < 0.05$; **, $0.001 \leq p < 0.05$; ***, $p < 0.001$.
980 **Table 1** Summary statistics from mixed linear models (LMMs) assessing a subset of
981 performance and fitness traits for *Col*, CS864818 (*wkry38*) and CS68738 (*lsd1*) under well-
982 watered and drought conditions during the main drought screen. Each LMM independently
983 analyzes *Col* and one mutant (either *wrky38* or *lsd1*). β represents the estimated effect size, and
984 subscripts indicate effects attributed to genotype (G), treatment (Trt) or genotype-by-treatment
985 interaction (GxTrt); *p* represents the *p*-value at $\alpha = 0.05$, and p_{adj} represents the adjusted *p*-value
986 at FDR = 0.05. A negative β_G reflects a lower trait value in the mutant compared to *Col*, while a
987 positive β_{Trt} reflects a lower trait value under drought compared to well-watered conditions.
988 **Table 2** Summary statistics from mixed linear models (LMMs) assessing a subset of
989 performance and fitness traits for *Col*, CS864818 (*wkry38*) and CS68738 (*lsd1*) under well-
990 watered and intermediate drought (ID) conditions during the follow-up intermediate drought
991 experiment. Each LMM independently analyzes *Col* and one mutant (either *wrky38* or *lsd1*). β
992 represents the estimated effect size, *p* represents the *p*-value at $\alpha = 0.05$, and subscripts
993 indicate effects attributed to genotype (G), treatment (Trt) or genotype-by-treatment interaction
994 (GxTrt). A negative β_G reflects a lower trait value in the mutant compared to *Col*, while a positive
995 β_{Trt} reflects a lower trait value under ID compared to well-watered conditions.

996 Author contributions

997 YL, CML, and JRL designed the study, CL and YL performed experiments, YL conducted data
998 analyses, YL, ELP, and JRL interpreted results, YL, CML, and JRL wrote the manuscript, all
999 authors edited and approved the manuscript.

1000 Figures and Tables

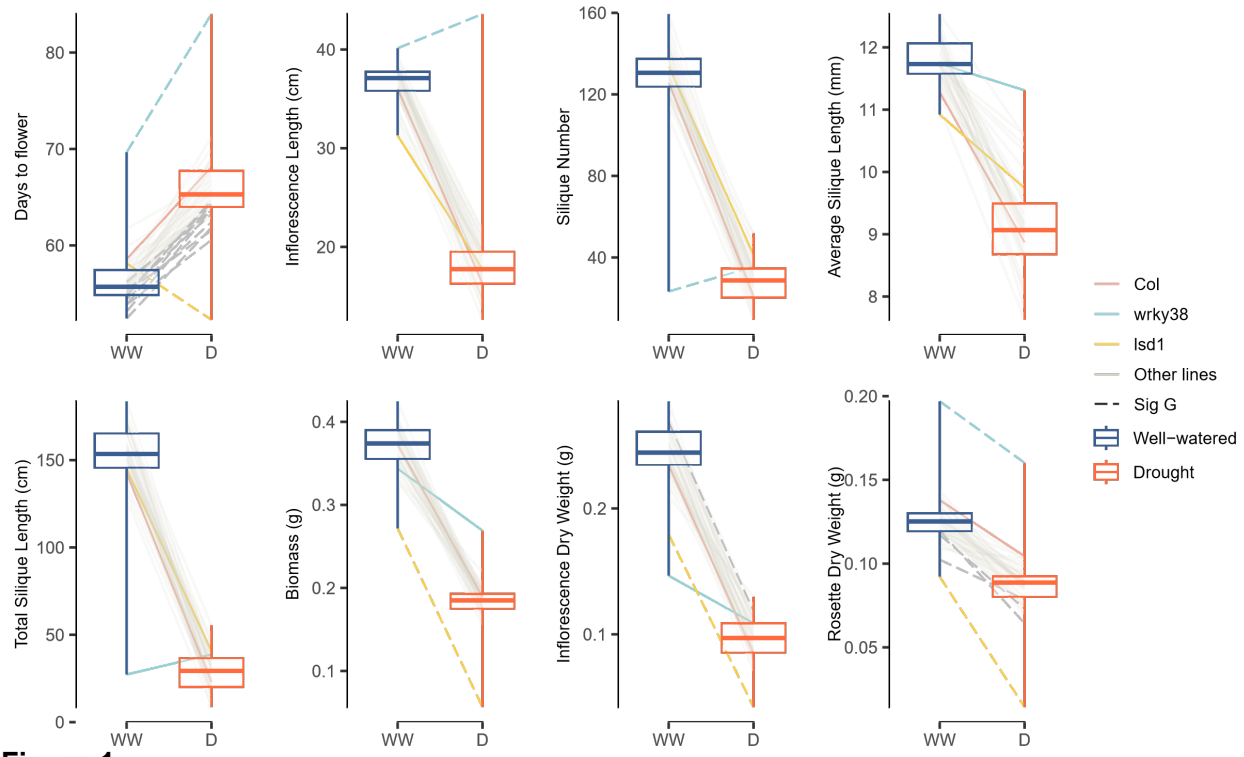

Figure 1

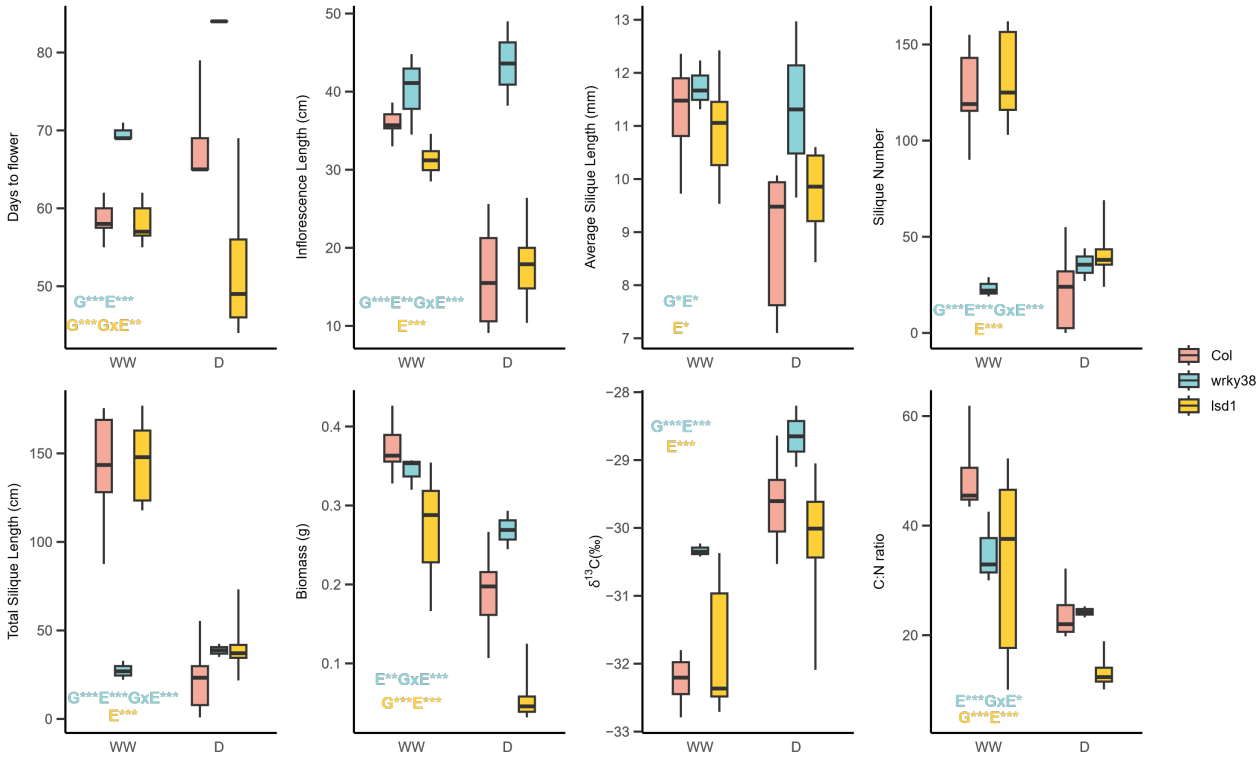

Figure 2

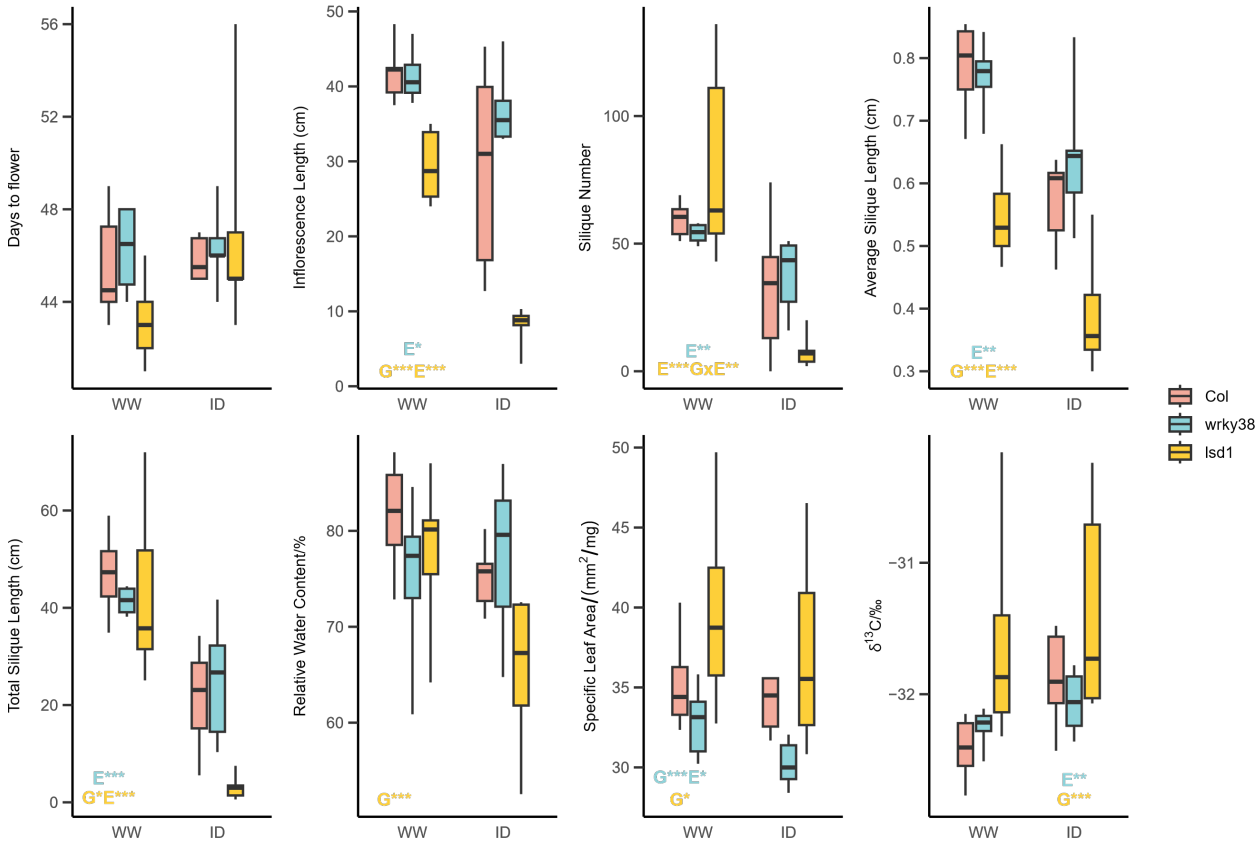
Days to flower
Inflorescence Length (cm)
Silique Number
Average Silique Length (cm)
Total Silique Length (cm)
Relative Water Content/%
Specific Leaf Area/(mm²/mg)
δ13C/‰
WW
ID
E*
G***E***
E**
E***GxE**
E**
G***E***
E***
G*E***
G***
G***E*
G*
E**
G***
Col
wrky38
lsd1

Figure 3

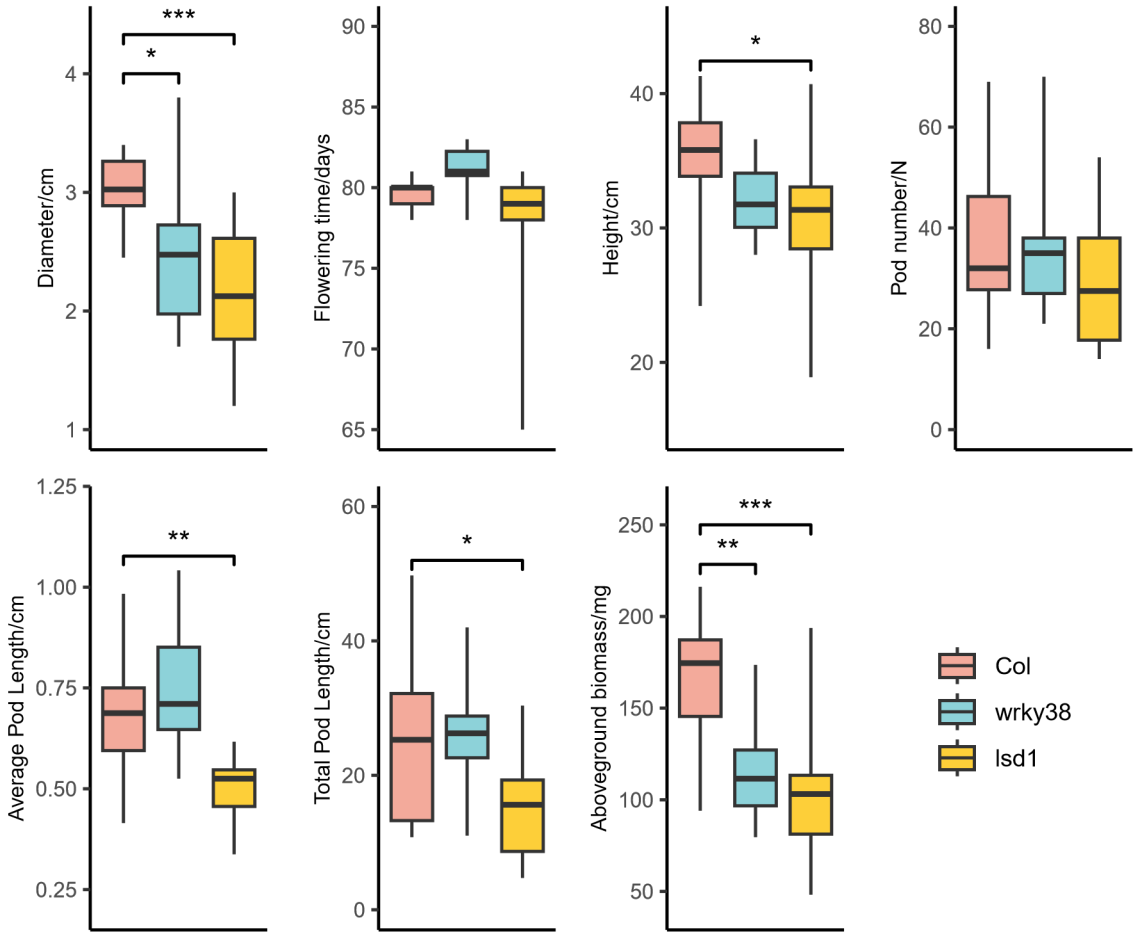
Diameter/cm
Flowering time/days
Height/cm
Pod number/N
Average Pod Length/cm
Total Pod Length/cm
Aboveground biomass/mg
Col
wrky38
lsd1

Figure 4

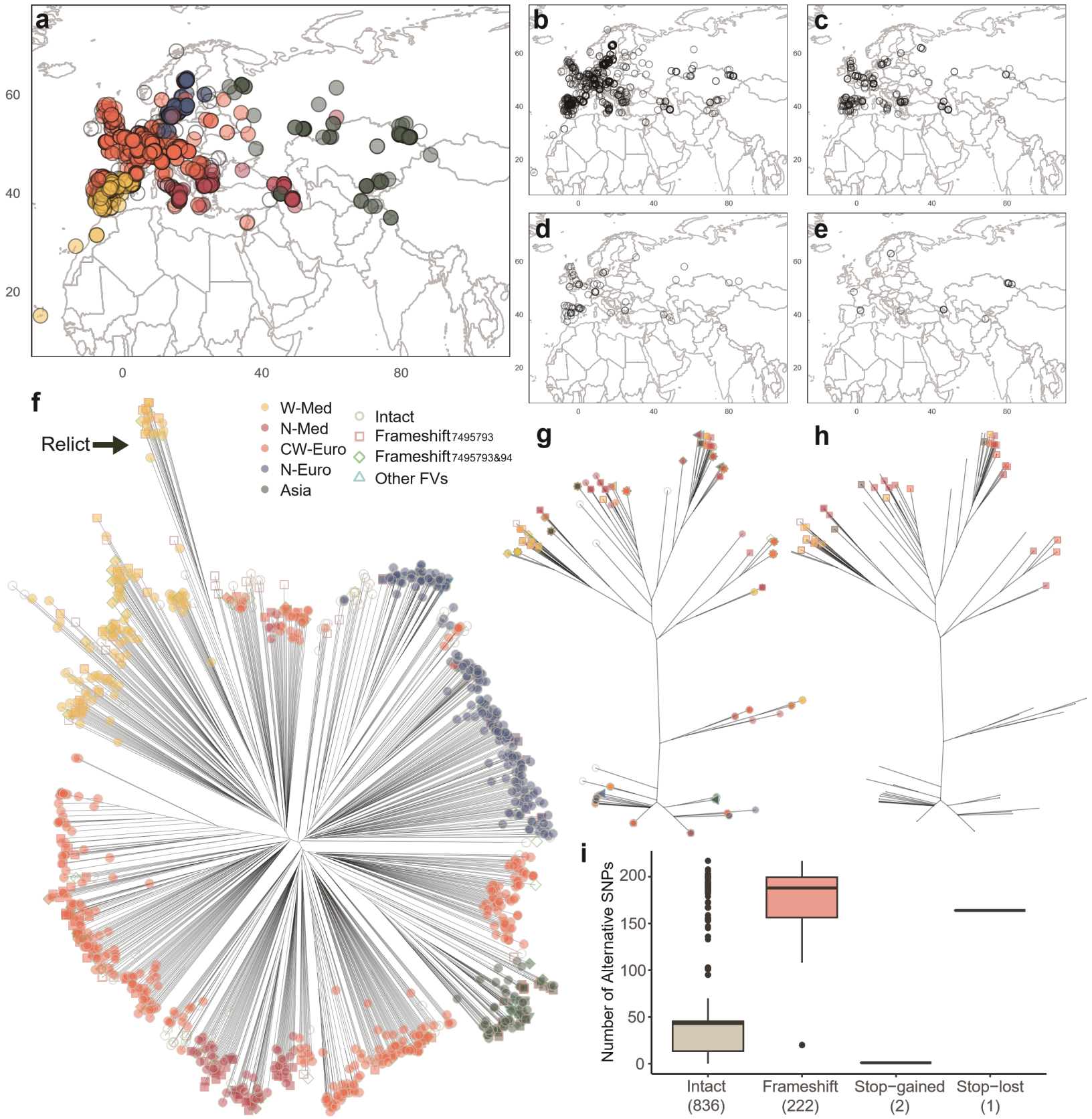

1012 **Figure 5**

1013

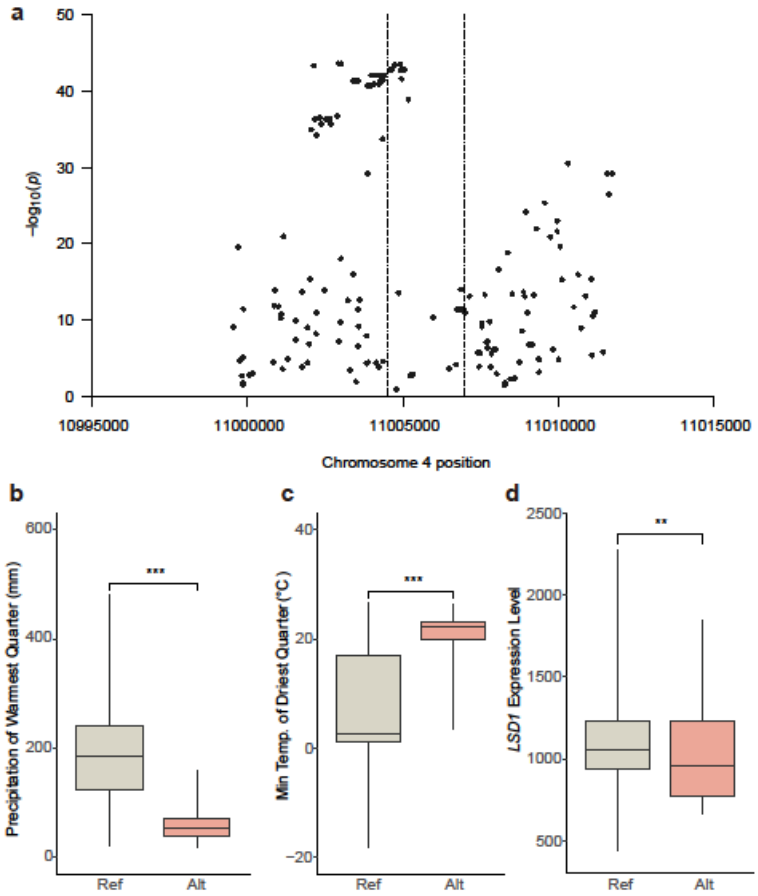
a
50
40
30
20
10
0
−log10(p)
10995000
11000000
11005000
11010000
11015000
Chromosome 4 position
b
600
400
200
0
Precipitation of Warmest Quarter (mm)
***
Ref
Alt
c
40
20
0
−20
Min Temp. of Driest Quarter (°C)
***
Ref
Alt
d
2500
2000
1500
1000
500
LSD1 Expression Level
**
Ref
Alt

Figure 6

1026 **Table 1**

Col-CS864818 (*wkry38*)	Genotype Effect			Treatment Effect			Genotype-by-Treatment		
	β_G	*p*	p_{adj}	β_{Trt}	*p*	p_{adj}	β_{GxTrt}	*p*	p_{adj}
Days to Flower (days)	15.86	**<0.0001**	**0.0002**	-9.57	**<0.0001**	**<0.0001**	-4.76	0.2380	0.8081
Inflorescence Length (cm)	27.33	**<0.0001**	**0.0014**	19.74	**0.0086**	**0.0086**	-23.21	**0.0006**	**0.0274**
Total Silique Length (cm)	15.82	**0.0018**	0.0782	120.03	**0.0009**	**0.0009**	-131.47	**0.0002**	**0.0076**
Biomass (g)	0.08	0.6793	0.9218	0.18	**0.0059**	**0.0059**	-0.14	**0.0004**	**0.0189**
Col-CS68738 (*lsd1*)	Genotype Effect			Treatment Effect			Genotype-by-Treatment		
	β_G	*p*	p_{adj}	β_{Trt}	*p*	p_{adj}	β_{GxTrt}	*p*	p_{adj}
Days to Flower (days)	-15.86	**0.0009**	**0.0082**	-9.57	0.3981	0.3981	15.43	**0.0015**	0.0675
Inflorescence Length (cm)	19.74	0.3586	0.6422	-6.20	**<0.0001**	**<0.0001**	20.14	0.0852	0.9698
Total Silique Length (cm)	17.75	0.2947	0.6362	120.03	**<0.0001**	**<0.0001**	-15.68	0.4049	0.9684
Biomass (g)	-0.13	**<0.0001**	**<0.0001**	0.18	**<0.0001**	**<0.0001**	0.03	0.4058	0.7440

1027 Note: *p*-values less than 0.05 are presented in bold to indicate statistical significance.

1028

1029 **Table 2**

Col-CS864818 (*wkry38*)	β_G	p_G	β_{Trt}	p_{Trt}	β_{GxTrt}	p_{GxTrt}
Days to Flower (days)	0.50	0.1503	-0.33	0.9684	0.93	0.4626
Inflorescence Length (cm)	7.75	0.2416	12.67	**0.0105**	-8.11	0.2551
Silique Number	5.00	0.9632	26.67	**0.0023**	-10.50	0.4705
Total Silique Length (cm)	3.63	0.8752	25.68	**<0.0001**	-9.23	0.2925
Specific Leaf Area (mm^2/mg)	-3.80	**0.0005**	1.19	**0.0313**	1.43	0.4181
Col-CS68738 (*lsd1*)	β_G	p_G	β_{Trt}	p_{Trt}	β_{GxTrt}	p_{GxTrt}
Days to Flower (days)	1.42	0.7466	-0.33	0.1908	-3.63	0.1365
Silique Number	-25.00	0.8293	26.67	**0.0007**	48.51	**0.0081**
Inflorescence Length (cm)	-21.10	**<0.0001**	12.67	**<0.0001**	8.65	0.1897
Total Silique Length (cm)	-18.25	**0.0234**	25.68	**<0.0001**	14.45	0.1378
Specific Leaf Area (mm^2/mg)	3.11	0.0368	1.19	0.4479	1.41	0.6989

1030 Note: *p*-values less than 0.05 are presented in bold to indicate statistical significance.